

Spring 2012

Investigation of chromophoric dissolved organic matter as a freshwater tracer in the Kennebec River Estuary

Alison Barner

University of New Hampshire, Durham

Follow this and additional works at: <https://scholars.unh.edu/thesis>

Recommended Citation

Barner, Alison, "Investigation of chromophoric dissolved organic matter as a freshwater tracer in the Kennebec River Estuary" (2012).
Master's Theses and Capstones. 712.
<https://scholars.unh.edu/thesis/712>

This Thesis is brought to you for free and open access by the Student Scholarship at University of New Hampshire Scholars' Repository. It has been accepted for inclusion in Master's Theses and Capstones by an authorized administrator of University of New Hampshire Scholars' Repository. For more information, please contact nicole.hentz@unh.edu.

**INVESTIGATION OF CHROMOPHORIC DISSOLVED ORGANIC
MATTER AS A FRESHWATER TRACER IN THE
KENNEBEC RIVER ESTUARY**

by

ALISON BARNER

B.S., University of Washington, 1993

M.L.I.S., University of Illinois at Urbana-Champaign, 2002

THESIS

Submitted to the University of New Hampshire

in Partial Fulfillment of

the Requirements for the Degree of

Master of Science

in

Earth Sciences: Oceanography

May 2012

UMI Number: 1518017

All rights reserved

INFORMATION TO ALL USERS

The quality of this reproduction is dependent upon the quality of the copy submitted.

In the unlikely event that the author did not send a complete manuscript and there are missing pages, these will be noted. Also, if material had to be removed, a note will indicate the deletion.

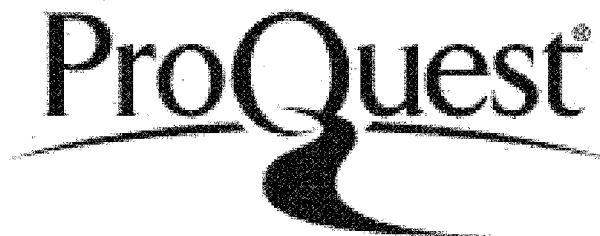


UMI 1518017

Published by ProQuest LLC 2012. Copyright in the Dissertation held by the Author.

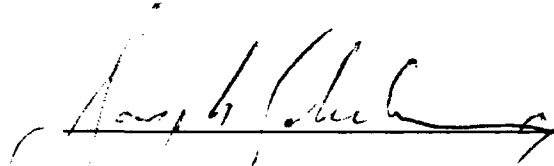
Microform Edition © ProQuest LLC.

All rights reserved. This work is protected against unauthorized copying under Title 17, United States Code.

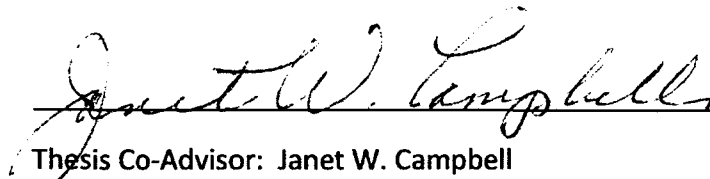


ProQuest LLC
789 East Eisenhower Parkway
P.O. Box 1346
Ann Arbor, MI 48106-1346

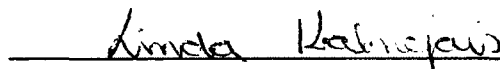
This thesis has been examined and approved.



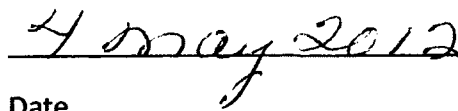
Thesis Co-Advisor: Joseph E. Salisbury
Research Assistant Professor/Affiliate Assistant Professor
Ocean Process Analysis Laboratory and
Earth Sciences Department



Thesis Co-Advisor: Janet W. Campbell
Research Professor Emerita
Ocean Process Analysis Laboratory and
Earth Sciences Department



Linda H. Kalnejais
Assistant Professor
Earth Sciences Department and
Ocean Process Analysis Laboratory



Date

ACKNOWLEDGMENTS

Many thanks to my advisor Janet Campbell for her astute advice and guidance, her insight and knowledge, and the numerous hours she spent helping me to research, write, and organize this thesis. This thesis would not have been possible without her assistance. I feel very fortunate to have her as an advisor.

I would like to thank my advisor Joe Salisbury for his intriguing suggestions and direction regarding the research for this thesis, and for his critique of the thesis draft. I would like to thank Thesis Committee member Linda Kalnejais for her comments and critique of the thesis draft as well.

I would like to express my gratitude to Chris Hunt for preparing the UNH COOA dataset for my use.

Thank you to my family and all the people who supported me during this endeavor.

TABLE OF CONTENTS

ACKNOWLEDGMENTS.....	iii
LIST OF TABLES.....	v
LIST OF FIGURES.....	vi
ABSTRACT.....	viii
1 INTRODUCTION	1
2 DERIVING CDOM ABSORPTION FROM FDOM	13
COOA Data Collection and Instrumentation.....	14
Data Extraction for Thesis.....	17
Data Analysis.....	19
Results and Discussion	20
3 INVESTIGATING CDOM AS A TRACER OF FRESHWATER	36
Data and Methods	38
Results.....	40
Discussion.....	42
Conclusions	45
4 FINAL WORDS.....	57
REFERENCES	60

List of Tables

Table 1. Cruise date, station range and number, FDOM and spec ag412 mean and standard deviation, slopes, intercepts and R^2 from spec linear regressions, and standard error for all 14 cruises.....	22
Table 2. Cruise date, station range and number, FDOM and prof agp412 mean and standard deviation, slopes, intercepts and R^2 from prof linear regressions, and standard error for all 14 cruises.....	22
Table 3. Variability in FDOM, ag412, and the ratio of FDOM to ag412 at each station sampled in the COOA Coastal Transect. Shown here are the number of observations (N), and the mean, standard deviation (stdev), and coefficient of variation (CV) of these variables at each station.	23
Table 4. Cruise date with corresponding Julian day, daily discharge, cumulative discharge, average discharge, and discharge difference in ft^3/s for all 14 cruises.	47
Table 5. Salinity levels at stations 4, 5, and 6 for each of the 14 cruises.	47
Table 6. Cruise date with corresponding Julian day, ag412 at salinity=0, ag412 at maximum salinity, maximum salinity (PSU), ag412 at salinity=15 PSU, and ΔCDOM for all 14 cruises.	48

List of Figures

1. Watersheds in Maine and map showing the 6 stations of the UNH COOA Coastal Transect cruise track	12
2. Graph for February 17, 2005 cruise showing $ag(\lambda)$ vs. FDOM at 3 different wavelengths: 412, 443, and 490 nm.....	24
3. Spectral slopes for $ag(\lambda)$ data at each COOA Coastal Transect station.....	25
4. Absorption coefficients, ag_{412} (blue) and agp_{412} (red), plotted against FDOM for all stations in the database.....	26
5. Calibration regression data for September 24, 2004 cruise.	27
6. Calibration data for November 4, 2004.....	27
7. Calibration data for February 17, 2005.....	28
8. Calibration data for June 29, 2005.....	28
9. Calibration data for August 17, 2005.....	29
10. Calibration data for February 22, 2006.....	29
11. Calibration data for July 19, 2006.....	30
12. Calibration data for September 15, 2006.....	30
13. Calibration data for December 14, 2006.	31
14. Calibration data for May 7, 2007.....	31
15. Calibration data for June 19, 2007.....	32
16. Calibration data for August 21, 2007.....	32
17. Calibration data for November 13, 2007.....	33
18. Calibration data for January 16, 2008.....	33

19. Spectrophotometer ag412 vs. FDOM color-coded by Coastal Transect station number.....	34
20. Profiler agp412 vs. FDOM color-coded by Coastal Transect station number.	35
21. CDOM absorption coefficient vs. salinity for COOA Coastal Transect cruises in 2004 and 2005.	49
22. CDOM absorption coefficient vs. salinity for COOA Coastal Transect cruises in 2006.	50
23. CDOM absorption coefficient vs. salinity for COOA Coastal Transect cruises in 2007 and 2008.	51
24. Schematic illustrating Δ CDOM representing departure from a conservative mixing line.	52
25. Δ CDOM vs. Julian Day for the 14 COOA Coastal Transect cruises.....	53
26. Δ CDOM vs. Daily Discharge for the 14 Coastal Transect cruises.....	54
27. Δ CDOM vs. Average Discharge for the 14 Coastal Transect cruises.	55
28. Δ CDOM vs. Discharge Difference for the 14 Coastal Transect cruises.....	56

ABSTRACT

INVESTIGATION OF CHROMOPHORIC DISSOLVED ORGANIC MATTER AS A FRESHWATER TRACER IN THE KENNEBEC RIVER ESTUARY

by

Alison Barner

University of New Hampshire, May, 2012

In an attempt to explore the feasibility of using chromophoric dissolved organic matter (CDOM) as a freshwater tracer in the Kennebec Estuary of Maine, potential causes of the variability of the CDOM absorption coefficient (a_{g412}) in relation to salinity were investigated. A predictable relationship between CDOM variability and factors such as river discharge and season was sought to explain CDOM variability for use in remote sensing. To accomplish these objectives, a_{g412} was calibrated to continuous underway FDOM measurements using linear regressions from 14 cruises. USGS daily discharge rates were checked for possible relationships with a_{g412} values. Although no trends were noted, there were elevated CDOM accumulation levels during summer suggestive of summer salt marsh growth. A residence time hypothesis is described to explain the relationship between discharge rates and CDOM accumulation levels in the estuary. The absence of trending in the data suggests that CDOM variability is complex and influenced by multiple factors.

CHAPTER 1

INTRODUCTION

Chromophoric or colored dissolved organic matter (CDOM) plays an important role in the surface waters of coastal and marine areas. CDOM has a substantial effect on the amount of light available for photosynthesis in all natural waters. Due to its ability to absorb sunlight, CDOM affects the optical properties and biogeochemistry of surface waters, and because of its influence on the water's optical properties, it can be mapped using remote sensing techniques (Mannino et al. 2008). In addition, because CDOM occurs in higher levels in freshwater than saltwater, it is potentially useful as a freshwater tracer (DelCastillo and Miller 2008; Salisbury et al. 2011).

Among the reasons for tracing freshwater is the desire to quantify the export of carbon from the land to the ocean in studies of the global carbon cycle (Hopkinson et al. 1998; Liu et al. 2000; Salisbury 2009). With more study, people can understand more precisely how CDOM varies in freshwater, and its relationship to dissolved organic carbon (DOC). Hence the subject of this thesis: to investigate the variability of CDOM and its possible use as a tracer of freshwater in the Kennebec Estuary entering the western Gulf of Maine.

Chromophoric dissolved organic matter (CDOM) is the fraction of dissolved organic matter (DOM) that strongly absorbs ultraviolet (UV) and short-wavelength visible light (Twardowski et al. 2001; Helms et al. 2008). It exists in all natural waters due to the degradation of both terrestrial and aquatic plant material (Stedmon and Markager 2001). Although DOM is analogous to dissolved organic carbon (DOC), the relationship of DOC to CDOM is variable (Novak 2004). Its absorption decreases exponentially with increasing wavelength of light according to the expression (Bricaud et al. 1981):

$$a(\lambda) = a(\lambda_0) \exp[-S(\lambda - \lambda_0)] \quad (1.1)$$

where $a(\lambda)$ and $a(\lambda_0)$ are the absorption coefficients at wavelength λ and a reference wavelength λ_0 , respectively, and the spectral slope S defines how quickly the absorption decreases with increasing wavelength. Because different types of CDOM have different spectral slopes, S can potentially be used to characterize CDOM (Helms et al. 2008).

Absorption coefficients are derived from the relation,

$$a(\lambda) = 2.303 A(\lambda)/r \quad (1.2)$$

where A is the optical density measured across pathlength, r (Blough and Del Vecchio 2002). This research uses $\lambda_0=412$ nanometers (nm), and we denote the CDOM absorption coefficient at 412 nm as a_{g412} , in which the “ g ” refers to *gelbstoff*, a German word meaning “yellow substance”, referring to CDOM (Kirk 1983).

The composition of CDOM differs depending upon its source. Terrestrially-derived CDOM from rivers or runoff contains a large proportion of organic acid polymers called humic and fulvic acids, which are formed during decomposition of plant matter. This material travels to the sea via rivers and groundwater inputs (Twardowski and Donaghay 2001). Open ocean or marine CDOM chiefly contains marine humic and fulvic acids possibly created from reactions of fatty acids released by phytoplankton (Harvey and Boran 1985; Carder et al. 1989). Phytoplankton production is another process that gives rise to CDOM, but it is of secondary importance as a source of CDOM within estuaries (Blough and Del Vecchio 2002).

Removal of CDOM from the water column occurs through different mechanisms. Examples of removal mechanisms include adsorption (or physical attachment) onto particles, flocculation followed by precipitation, bacterial decomposition, and breakdown via photochemical oxidation or photobleaching (Stedmon and Markager 2001). Photobleaching, or photodegradation by UV light, is the most important CDOM sink in coastal waters; this removal process breaks down CDOM into smaller, colorless molecules (Romera-Castillo et al. 2011).

CDOM from terrestrial sources enters the ocean by means of freshwater runoff, groundwater and sediment porewaters. So, CDOM can act as a tracer of freshwater because its concentration is higher in freshwater compared to saltwater. Salinity (or lack thereof) is used to trace freshwater land drainage to coastal areas. A linear relationship between salinity and CDOM absorption signifies conservative CDOM

behavior in that region. Nonlinear data indicates nonconservative CDOM behavior due to *in situ* sources or removal processes (Twardowski and Donaghay 2001). Since CDOM exhibits conservative behavior in many estuaries and coastal regions, it can be a good tracer of freshwater or salinity. This characteristic can be applied to remote sensing of CDOM, which can serve as a proxy for sea surface salinity measurements (Coble 1996; Gardner et al. 2005).

CDOM as a freshwater tracer can be used to quantify DOC fluxes from the land to the ocean. For example, a case study of the Yukon River, Alaska, showed a strong correlation between CDOM absorption and DOC concentrations in the Yukon River at Pilot Station (Spencer et al. 2009). Therefore, according to the results of that study, CDOM absorption measurements led to accurate DOC flux estimates from the Yukon River into the Arctic Ocean. Del Castillo and Miller (2008) found that using CDOM in remote sensing to trace the flow of the Mississippi River Plume also permitted estimates of DOC transport from the land to the Gulf of Mexico. However, Callahan et al. (2004) observed that the ratio of CDOM to DOC decreases with increasing salinity in the Pearl River Estuary of China, probably due to photobleaching of CDOM. In other words, the relationship of CDOM to DOC is variable, so the use of CDOM as a surrogate for DOC should be used with knowledge of the CDOM to DOC ratio. This kind of situation occurs along the continental shelf and slope area of the Mid-Atlantic Bight, where Mannino et al. (2008) used the first validated satellite retrieval algorithms to successfully retrieve coastal ocean surface DOC and CDOM absorption.

Because of its light absorption properties, CDOM affects biogeochemical processes and optics in surface waters (Vodacek et al. 1997). Since CDOM strongly absorbs short-wavelength blue light, including the light of the phytoplankton absorption peak near 440 nm, the presence of CDOM in the water column can decrease primary production by absorbing and diminishing photosynthetically available radiation (PAR) (Vodacek et al. 1997; Twardowski and Donaghay 2001). On the other hand, CDOM's light-absorbing properties can shield phytoplankton from harmful UVB radiation and increase photosynthesis (Vodacek et al. 1997; Stedmon and Markager 2001). Because CDOM and phytoplankton both absorb short-wavelength visible light, remote sensing applications of ocean color must separate the CDOM signal from the chlorophyll signal in order to accurately estimate chlorophyll concentrations. This task is currently problematic due to the limited knowledge of CDOM distributions in the oceans, especially along the coasts (Twardowski and Donaghay 2001).

An undetermined fraction of CDOM contains absorbing chromophores which also fluoresce or emit light; this subset of CDOM is often termed fCDOM (fluorescent CDOM) or FDOM (fluorescent dissolved organic matter) (Nelson and Siegel 2002). After excitation by light of a specific wavelength, fluorophores always emit light or fluoresce at a longer wavelength or lower energy than the excitation wavelength. Typically excitation maximum wavelengths are within the range of 300-400 nm, while emission maximum wavelengths usually fall between 400 and 500 nm (Blough and Del Vecchio 2002). According to Coble (1996), at least two different types of FDOM exist: a humic-like, gelbstoff fluorescence; and a protein- or amino acid-like fluorescence due possibly

in part to biological activity. The humic-like FDOM fluoresces at 420-450 nm after excitation at 230-260 and 320-350 nm. The tyrosine-like FDOM has an emission at 300-305 nm, while the tryptophan-like FDOM emits at 340-350 nm, both from excitation at 220 and 275 nm (Coble 1996).

Fluorescence measurements of FDOM can indirectly estimate CDOM absorption after determining a linear relationship between fluorescence and absorption for the specific geographical area of interest. Fluorescence measurements are generally more sensitive, faster and easier to make than CDOM absorption measurements; in addition, fluorescence measurements more readily allow for continuous *in situ* monitoring, resulting in high-resolution data (Nelson and Siegel 2002).

The fluorescence quantum yield, ϕ , is the ratio of light emitted as fluorescence to light absorbed (Blough and Del Vecchio 2002; Romera-Castillo 2011), or the fluorescence per unit absorbance. It can be represented by the equation:

$$\phi(\lambda_{ex}, \lambda_{em}) = F(\lambda_{em})/a(\lambda_{ex}) \quad (1.3)$$

where $F(\lambda_{em})$ is the integrated corrected fluorescence emission generated by excitation at wavelength λ_{ex} , and $a(\lambda_{ex})$ is the absorption coefficient at the excitation wavelength λ_{ex} (Green and Blough 1994).

The fluorescence quantum yield can compare the fluorescence efficiencies of different sources of CDOM, so it is another measure useful in characterizing and describing CDOM (Green and Blough 1994; Coble 2007). First demonstrated by Green

and Blough (1994), the fluorescence quantum yield varies little across waters from different regions, signaling a relatively linear relationship between CDOM fluorescence and absorption. Therefore, it is possible to use the fluorescence quantum yield and fluorescence measurements to obtain CDOM absorption coefficients (Blough and Del Vecchio 2002). Since fluorescence measurements are often continuous, and more rapid and sensitive than absorption measurements, this method for acquiring absorption measurements could prove desirable provided the fluorescence and absorption data relate linearly.

Measurement Techniques

Currently the standard method for measuring CDOM absorption is to use a conventional spectrophotometer (Green and Blough 1994). The spectrophotometer measures the optical density of filtered seawater samples in quartz-windowed cuvettes, and compares these measurements to those of a “blank”, which is a purified freshwater sample. The sensitivity or detection limit of CDOM absorption for this instrument is approximately 0.05 m^{-1} in 10 cm cells, which is close to the average absorption coefficient value of CDOM in the open ocean. Therefore, a major disadvantage of this technique is that it cannot accurately discern CDOM absorption levels in areas of low CDOM concentration (Nelson and Siegel 2002). Another drawback to spectrophotometry is that discrete sampling methods result in low-resolution profiles.

Another technique for measuring CDOM absorption employs *in situ* paired WETLabs AC-9 absorption meters first developed by Twardowski *et al.* (1999). One

meter estimates the CDOM absorption coefficient of a filtered water sample with particles larger than 0.2 μm filtered out; the signal from the filtered meter is subtracted from the unfiltered sample to estimate the particulate absorption coefficient. CDOM absorption is derived by subtracting the known absorption of pure seawater from the filtered sample measurement. This technique demonstrates two principal advantages over standard laboratory spectrophotometry: increased sensitivity and the generation of high-resolution profiles over a unit of time (Nelson and Siegel 2002).

Two important techniques measure FDOM fluorescent chromophore/fluorophore distribution patterns: synchronous fluorescence spectroscopy (Ferrari and Mingazzini 1995), and excitation-emission matrix (EEM) spectroscopy (Coble 1996). Synchronous fluorescence spectroscopy results in synchronous scan spectra generated by simultaneously scanning the excitation and emission wavelengths at a fixed wavelength difference. These spectra form two-dimensional plots (Blough and Green 1995).

EEM spectroscopy involves collecting repeated emission scans at various excitation wavelengths, and consolidating these scans into three-dimensional excitation-emission matrix spectra called EEMS (Coble 1996, 2007). The EEMS can be expressed as a topographic plot with the excitation and emission wavelengths representing two axes, and the convergence of these two spectra resulting in the fluorescence intensity on the z axis (Coble 1996). A new parameter achieved by the use of EEM spectroscopy is the wavelength-independent fluorescence maximum ($Ex_{\text{max}}/Em_{\text{max}}$) of a sample; each matrix

automatically reveals the maximum fluorescence obtained by a certain unique combination of excitation and emission wavelengths (Coble 1996). As opposed to single-scan techniques, EEM spectroscopy obviously presents much more information and more complete FDOM emission spectra, which can help to distinguish between different classes of fluorophores, and therefore aid in categorizing different emitting species of FDOM (Coble 1996; Blough and Del Vecchio 2002).

Seasonal variability of CDOM

The amount of CDOM entering a river varies substantially over the course of a year. This thesis addresses the question: What controls seasonal variability of CDOM in a river? Or, rephrasing the question: Why are riverine CDOM levels so highly variable from season to season and from year to year? Certain environmental factors, if present in the area, have the potential to raise or lower the amount of CDOM entering a river system. For example, the watershed yields differing amounts of CDOM depending upon the soil type adjacent to the river; even fallen leaves and other detrital matter increase CDOM levels as rainwater runs over the ground to the river. Another possibility is the dilution of river water by stormflow. A lot of rain dilutes the water entering a river, thereby clarifying the water and decreasing CDOM levels in the river. Finally, the amount of sunlight entering the water column impacts the degree of photobleaching of CDOM. Photobleaching inhibits the ability of CDOM to absorb light by destroying the chromophores in DOM, resulting in less CDOM in the water column. These factors provide speculation for the causes of riverine CDOM variability.

To investigate the variability of CDOM and its possible use as a freshwater tracer in the Kennebec Estuary, this research uses datasets from the 2004-2008 University of New Hampshire (UNH) Coastal Ocean Observing and Analysis (COOA) Coastal Transect (CT) cruises. These cruises began at the mouth of the Piscataqua River by Portsmouth, NH, traveled north along the coast of the Gulf of Maine, and then headed up the Kennebec Estuary in Maine before returning to Portsmouth (Figure 1).

The Kennebec Estuary is formed at Merrymeeting Bay by the convergence of the Kennebec and Androscoggin Rivers. The Androscoggin River was designated one of the ten most polluted rivers in America in the 1960s (Mitnik 2002), and both rivers have a history of water-quality problems. Numerous pulp and paper mills are located along the rivers, as well as municipal wastewater treatment facilities. Prior to the passage of the Clean Water Act in 1972, partially treated and untreated municipal and industrial wastewater was discharged directly into both rivers. Clean-up activities since that time have partially restored the Androscoggin, and now it is possible to fish and swim in both rivers (Hunt 2002).

The Kennebec Estuary was a focus of the COOA field work for five years (2004-2008). Discharge from this estuary mixes with the Western Maine Coastal Current and is carried southward, thus potentially affecting water conditions throughout the region. The COOA Coastal Transect cruises collected water samples and made vertical profile measurements at fixed stations along the transect, and operated a continuous flow-through system measuring FDOM fluorescence, temperature, salinity, and other

properties between stations. The flow-through fluorescence (FDOM) data were used to derive continuous CDOM absorption coefficient (ag412) values for these CT cruises. Seasonal variability observed in the CDOM absorption data was studied to determine whether it is governed by river discharge or other environmental factors. In addition, the possibility of using CDOM as a tracer of freshwater was investigated with the use of the flow-through salinity data.

In Chapter 2, results of converting fluorescence to ag412 are presented. Chapter 3 presents ag412 vs. salinity graphs and investigates their relationship to discharge. Nonlinearity is also explored and possible explanations are described in Chapter 3. Finally, Chapter 4 describes future directions to be taken in this work.

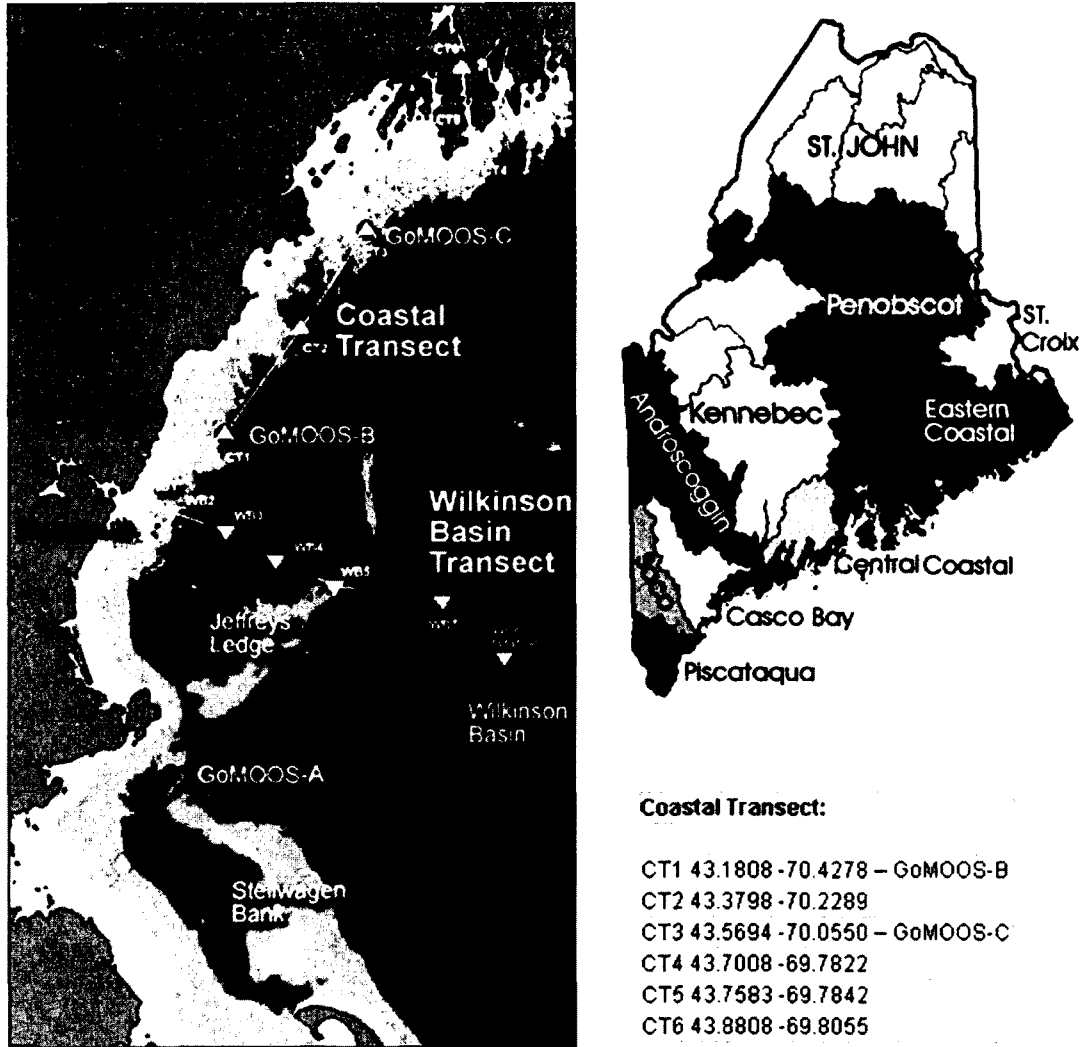


Figure 1. Watersheds in Maine (upper right) and map (left) showing the 6 stations of the UNH COOA Coastal Transect cruise track beginning near Portsmouth, New Hampshire, and traveling along the Gulf of Maine coast and up the Kennebec Estuary in Maine. The latitude and longitude coordinates of each CT station are given in the legend.

Image source: http://www.cooa.unh.edu/data/boats/coastal_wilkinson_sampling_locations.jpg Watersheds from <http://mainerivers.org/watershed-profiles/>.

CHAPTER 2

DERIVING CDOM ABSORPTION COEFFICIENT FROM FDOM

This chapter explores the feasibility of using continuous fluorescence measurements of FDOM to obtain the CDOM absorption coefficient by investigating the relationship between fluorescence and CDOM absorption on COOA Coastal Transect (CT) cruises. Successful results would encourage using FDOM measurements to obtain CDOM absorption; this would increase efficiency in retrieving CDOM absorption data because FDOM readings can be collected more easily, quickly and thoroughly than CDOM absorption measurements. In order to accomplish this objective, CDOM absorption coefficients measured by a spectrophotometer were calibrated to flow-through FDOM data from each cruise using linear regressions. As a measure of quality control, the CDOM absorption measurements were compared with measurements of CDOM and particle absorption made by a profiler. The methods used to collect the COOA data are described in the following section.

COOA Data Collection and Instrumentation

Spectrophotometer measurements were made in the laboratory from seawater samples collected on cruises. The “bottle data” were collected at fixed stations and depths using 5-liter Niskin bottles raised onboard the UNH research vessel *Gulf Challenger*. Samples were poured into opaque brown 500-ml plastic bottles and taken to the ship’s lab below deck for filtration. Per the NASA/SIMBIOS protocols (Mitchell et al. 2003), the CDOM sample filtration process uses a glass filtration set-up with a glass vacuum flask attached to a vacuum pump, and a funnel with a 0.22- μm Millipore Durapore filter¹ and stainless steel frit (or mesh) placed on top of the flask. The flask and funnel were triple-rinsed in distilled deionized water (DDW) before triple-rinsing the funnel with the sample. Then the flask was triple-rinsed with 20-30 ml of filtrate drawn by the vacuum pump into the flask. Finally, after the water samples from the brown plastic bottles were filtered into the flask, about 60-75 ml of filtrate was poured from the flask into a 125-ml opaque brown borosilicate glass bottle. This bottle was acid-washed, triple-rinsed and stored with DDW before use. Then the bottle with the filtrate was kept on ice until it was refrigerated in the OPAL laboratory. The bottle stayed in the refrigerator anywhere from several days up to two weeks until a full batch of samples were ready to run on the spectrophotometer.

Absorption measurements were made on the bottle water samples in the OPAL laboratory using a Perkin Elmer Lambda 800 UV-VIS spectrophotometer (Waltham,

¹ CDOM is defined operationally as the absorption coefficient of the filtrate, and hence it may also be influenced by very small particles that pass through a 0.22- μm filter.

Massachusetts). This instrument measures absorbance for wavelengths between 200 and 800 nm at 1-nm intervals. The spectrophotometer is equipped with a light source, a grating which separates the light into different wavelengths, two cuvette holders, and a motor. This instrument uses two glass cuvettes with a pathlength of 10 cm, one cuvette for the standard and one for the sample. The control or standard is calibrated across the entire spectrum twice before use. Then, a single reading from each sample is taken; if there is a problem, multiple readings of the sample are taken, and either the most accurate reading or an average of the readings is used. The spectrophotometer measures the visible and ultraviolet light absorbance of the sample (in this case, the CDOM sample), which is indicated by the amount of light attenuated as the light is passed through the seawater sample inside the cuvette. A computer converts absorbance to absorption coefficients and displays the absorption spectra of the samples, which are saved in an ASCII file that automatically provides the wavelengths used by the instrument. Finally, the absorption coefficient spectra are processed with a MATLAB code, and negative exponential curves are fitted to the processed CDOM absorption spectra to estimate the spectral slope (S).

Profiler data include measurements of inherent optical properties (IOPs) made in the vertical water column at each station. The profiler system is composed of several instruments contained within a cage which is lowered into the water to selected depths to make measurements. Before use, the profiler is always cleaned with methanol and calibrated, and the optical sensor is flushed with DDW. The OPAL profiler is a WETLabs setup equipped with the following instruments: WETLabs AC-S (Philomath, Oregon),

WetStar (Philomath, Oregon), SeaBird SBE-49 CTD, SeaBird SBE-43 oxygen sensor, DH-4 datalogger, and a battery. After the profiler is submerged, water enters 2 intake tubes connected to the AC-S, which makes absorbance (A) and attenuation (C) measurements with 1 reflecting tube and 1 absorbing tube inside the instrument. Then this water flows through a tube to the oxygen sensor and finally into a pump, where the water is pumped out of the profiler. The WetStar contains 2 *in-situ* fluorometers which measure CDOM and chlorophyll fluorescence as a proxy for CDOM and chlorophyll a. The SeaBird CTD takes conductivity (or salinity) and temperature measurements at selected depths. This research only uses profiler data obtained at a depth of 2 meters, which roughly coincides with the surface Niskin bottle and flow-through depths. However, the *Gulf Challenger* profiler data has been processed to generate readings every 0.5 m in depth throughout the water column.

A **flow-through system** onboard the *Gulf Challenger* obtained continuous measurements of salinity, temperature, stimulated fluorescence of CDOM (FDOM), and stimulated fluorescence of chlorophyll (FCHL). Water was pumped from approximately 1.0 m depth at a rate of 3.5 liters per minute to the shipboard flow-through equipment, where measurements were made once per second. The data were sub-sampled at 20-second intervals. Water entered the flow-through system through a manifold that controls the flow rate of the water through the tubes. One tube guided water to the optical instruments, in this case the WETLabs WETStar fluorometers, which measured FDOM (ex/em: 370/460 nm) and FCHL (ex/em: 460/695 nm). Before the water reached the fluorometers, a vortex debubbler removed bubbles from the water.

Another tube moved water to the Seabird SBE 45 CTD, which measured salinity and temperature.

All COOA data are stored in a database called the Uberstructure. This data structure contains measurements from the bottle or discrete spectra, underway flow-through system, and vertical profiler. For each station on each cruise, there exists an entry in the Uberstructure with all appropriate cruise data for that particular location and time matched to that entry. The Uberstructure contains data for 31 COOA Coastal Transect (CT) cruises between September 2004 and January 2008.

Data Extraction for Thesis

Data from the CT cruises were extracted from 6 stations in the Gulf of Maine and the Kennebec River Estuary (Figure 1) by UNH research scientist Chris Hunt using a MATLAB code that matched flow-through data at each station with the corresponding surface Niskin bottle and 2-meter profiler data. Absorption measurements from the spectrophotometer and vertical profiler were extracted at four wavelengths (412, 443, 490 and 676 nm). Chris Hunt also extracted cruise parameters such as latitude, longitude, time, and date, as well as salinity and temperature from the flow-through system.

The extracted data were imported into an Excel spreadsheet and graphs of ag_{412} , ag_{443} , and ag_{490} versus FDOM for each cruise were created. Slopes, intercepts, and R^2 values were calculated. These values were used to compare the data with

stations and months of the year to determine whether any relationships or trends were apparent.

Figure 1 shows the location of each of the stations along the Coastal Transect cruise in the Gulf of Maine. The number of stations extracted for each cruise varied between 2 and 10 stations. Stations 1 through 6 correspond to the station numbers on figure 1. However, for some cruises, data were collected between stations or farther up-river than Station 6; in these cases, there are more than 6 stations on a cruise. Of the 31 Coastal Transect cruises in the database, there were nine cruises with only 2 stations and two with only 3 stations. These were eliminated from the analyses because trendlines in the graphs were too uncertain with so few points.

The profiler absorption measurements were compared with the spectrophotometer data as a measure of quality control. The profiler measures the absorption of particles in the water in addition to the CDOM, hence the “p” in agp412. Thus, its values should be higher than those measured by the spectrophotometer (henceforth called “spec”), which is only measuring the absorption of CDOM or “gelbstoff” in the filtered water samples. There were 3 cruises in which the profiler data were less than the spec data, and since it was impossible to know which data were correct, these cruises were eliminated.² In addition, 2 cruises were eliminated for which there were no profiler data. The profiler readings on the second day of a 2-day cruise on June 29-30, 2005

² One cruise, on October 26, 2007, had spec readings which were obviously in error since they were much higher than other data, perhaps due to an instrument malfunction on that day.

were eliminated because the profiler data on June 30 were too low compared to the first day of the cruise. Thus, only 14 cruises out of the original 31 remained for analysis.

Data Analysis

The data extracted for this research included the CDOM absorption coefficient at three different wavelengths: 412, 443, and 490 nm. The absorption coefficients at 443 and 490 nm are related to the coefficient at 412 nm by the spectral slope S (equation 1.1). Thus, the slopes and intercepts derived from linear regressions of $ag(\lambda)$ vs. FDOM (Figure 2) are related by the same exponential slope:

$$ag(\lambda) = m \exp[-S(\lambda - 412)] \text{ FDOM} + b \exp[-S(\lambda - 412)] \quad (2.1)$$

where m and b are the slope and intercept for the $ag(412)$ vs. FDOM regression. Since it is possible to derive results for 443 and 490 nm from equation (1.1) and the results acquired for 412 nm if the spectral slope S is known, the remainder of the research exclusively focuses on $\lambda_0=412$. Spectral slopes (S) were derived for $ag(\lambda)$ spectra by fitting linear equations to the data $\ln(ag(\lambda))$ vs. λ for wavelengths 412, 443, and 490 nm (Figure 3).

Linear regressions of ag_{412} vs. FDOM and agg_{412} vs. FDOM were performed for data from all 14 cruises. These linear regressions were generated using the trendline function in Excel and selecting first-order linear regressions. R^2 values were also derived using Excel. Slopes, intercepts and R^2 values were also calculated from standard

statistical formulae as a check and were found to agree with those derived from the Excel trendline function.

Results and Discussion

Regressions were computed for all spec and profiler data in the database (Figure 4). The lower R^2 values from these regression equations demonstrate the need for individual “calibration curves” for each cruise. Results of linear regressions or “calibration curves” for each of the 14 cruises are listed in Tables 1 and 2 and displayed in figures 5-18. (Please note that the scaling of both axes varies among the figures). Although the linear regressions had R^2 values greater than 0.90 for all but one cruise, they displayed variable slopes and intercepts.

An effort was made to relate variability in the slopes and intercepts to some type of pattern which can be explained by a physical reason. For example, an easily identifiable trend in a graph could show increasing $ag412$ values over time during a period of rising river discharge. An example of a seasonal trend in a slope would be high slope values in autumn and low slope values in late winter, possibly due to a CDOM increase in the Kennebec river system from leaf and detrital material washed into the river by fall rains. In the case of this research, the distribution of the slopes and intercepts for all cruises appeared random, did not form any consistent patterns, and could not be explained by any natural occurrence that was explored in the context of this thesis.

The linear regressions use the equation:

$$ag412 = m * FDOM + b \quad (2.2)$$

A positive y-intercept (positive b value) is potentially significant and possible to explain as non-FDOM material which absorbs light but does not fluoresce. Negative y-intercepts (negative b values) cannot be explained by physical conditions. However, the small negative intercepts in this research are probably not statistically significantly different from zero (J. Campbell, pers. comm.).

The slope variability appears to be strongly influenced by the wide range of absorption and fluorescence values at stations 5 and 6 (Figures 19 and 20). Variability in the slope is related to variability in the fluorescence yield (ϕ). Specifically,

$$\phi \approx 1/m \quad (2.4)$$

Thus, variations in the fluorescence yield in different geographical areas and under different environmental conditions would result in variable slopes for the linear regressions (Table 3). However, the observed variability in slopes (i.e., fluorescence yield) could not be associated with any obvious physical conditions. Nevertheless, the high R^2 values meant that the underway FDOM data could be used to derive CDOM absorption coefficients, as a proxy for CDOM, and to study its relationship to salinity. Results of that analysis are presented in the next chapter.

Table 1. Cruise date, station range and number, FDOM and spec ag412 mean and standard deviation, slopes, intercepts and R² from spec linear regressions, and standard error for all 14 cruises.

Cruise	Station Range	N	FDOM		Spec ag412		Spec ag412 vs FDOM			Std Err
			Mean	Stdev	Mean	Stdev	Slope	Intercept	R ²	
20040924	1 - 4	4	4.413	5.820	0.443	0.193	0.032	0.300	0.965	0.0019
20041104	1 - 6+	5	23.564	32.275	1.177	1.706	0.052	-0.059	0.984	0.0630
20050217	1 - 6	4	28.553	36.199	1.261	1.504	0.042	0.076	0.999	0.0032
20050629	3 - 6	4	31.879	29.393	2.182	2.092	0.070	-0.043	0.961	0.2536
20050817	1 - 6	4	14.507	18.581	0.980	1.085	0.058	0.134	0.997	0.0050
20060222	1 - 5	4	29.248	31.265	0.867	0.898	0.029	0.031	0.988	0.0149
20060719	3 - 6	4	29.938	24.236	1.879	1.605	0.066	-0.084	0.980	0.0737
20060915	1 - 6+	10	50.535	39.698	2.048	1.545	0.038	0.116	0.965	0.0941
20061214	2 - 6	5	9.696	17.961	1.499	1.812	0.099	0.539	0.962	0.1659
20070507	1 - 6	5	27.365	25.850	1.555	1.317	0.051	0.167	0.990	0.0232
20070619	1 - 5	5	8.537	4.550	0.565	0.180	0.036	0.259	0.827	0.0075
20070821	1 - 6	6	16.624	19.170	1.159	1.000	0.051	0.309	0.961	0.0492
20071113	1 - 6	4	25.210	39.113	1.345	1.902	0.049	0.119	0.999	0.0050
20080116	1 - 5	4	22.500	24.922	1.085	1.106	0.044	0.087	0.999	0.0018

Table 2. Cruise date, station range and number, FDOM and prof agp412 mean and standard deviation, slopes, intercepts and R² from prof linear regressions, and standard error for all 14 cruises.

Cruise	Station Range	N	FDOM		Prof agp412		Prof agp412 vs FDOM			Std Err
			Mean	Stdev	Mean	Stdev	Slope	Intercept	R ²	
20040924	1 - 4	4	4.413	5.820	0.585	0.236	0.040	0.406	0.991	0.0009
20041104	1 - 6+	5	23.564	32.275	1.319	2.023	0.062	-0.138	0.974	0.1517
20050217	1 - 6	4	28.553	36.199	1.385	1.866	0.051	-0.066	0.972	0.1479
20050629	3 - 6	5	31.879	29.393	2.260	2.385	0.079	-0.246	0.938	0.4706
20050817	1 - 6	4	14.507	18.581	1.120	1.348	0.073	0.069	0.999	0.0015
20060222	1 - 5	4	29.248	31.265	0.950	0.957	0.029	0.097	0.906	0.1330
20060719	1 - 6	5	24.489	24.269	1.975	2.012	0.081	-0.018	0.963	0.1993
20060915	1 - 6	6	28.731	36.262	1.690	1.813	0.050	0.261	0.990	0.0472
20061214	2 - 6	5	9.696	17.961	1.865	2.611	0.145	0.457	0.997	0.0246
20070507	1 - 6	5	27.365	25.850	1.819	1.876	0.072	-0.151	0.984	0.0721
20070619	1 - 5	5	8.537	4.550	0.617	0.257	0.050	0.190	0.781	0.0194
20070821	1 - 6	6	16.624	19.170	1.237	1.418	0.074	0.015	0.987	0.0308
20071113	1 - 6	4	25.210	39.113	1.814	2.575	0.066	0.154	1.000	0.0129
20080116	1 - 5	4	22.500	24.922	1.187	1.228	0.049	0.084	0.989	0.0264

Table 3. Variability in FDOM, ag412, and the ratio of FDOM to ag412 at each station sampled in the COOA Coastal Transect. Shown here are the number of observations (N), and the mean, standard deviation (stdev), and coefficient of variation (CV) of these variables at each station.

CT Station	N	FDOM			ag412			FDOM/ag412		
		mean	stdev	CV (%)	mean	stdev	CV (%)	mean	stdev	CV (%)
1	13	3.969	1.798	45%	0.434	0.401	92%	12.459	6.373	51%
2	4	3.941	2.235	57%	0.411	0.088	21%	9.178	3.895	42%
3	15	5.704	2.133	37%	0.434	0.142	33%	13.481	4.274	32%
4	15	16.018	8.592	54%	0.934	0.291	31%	18.300	9.549	52%
5	11	32.605	22.750	70%	1.496	0.931	62%	21.221	7.786	37%
6	10	67.660	18.069	27%	3.889	0.813	21%	17.787	4.810	27%

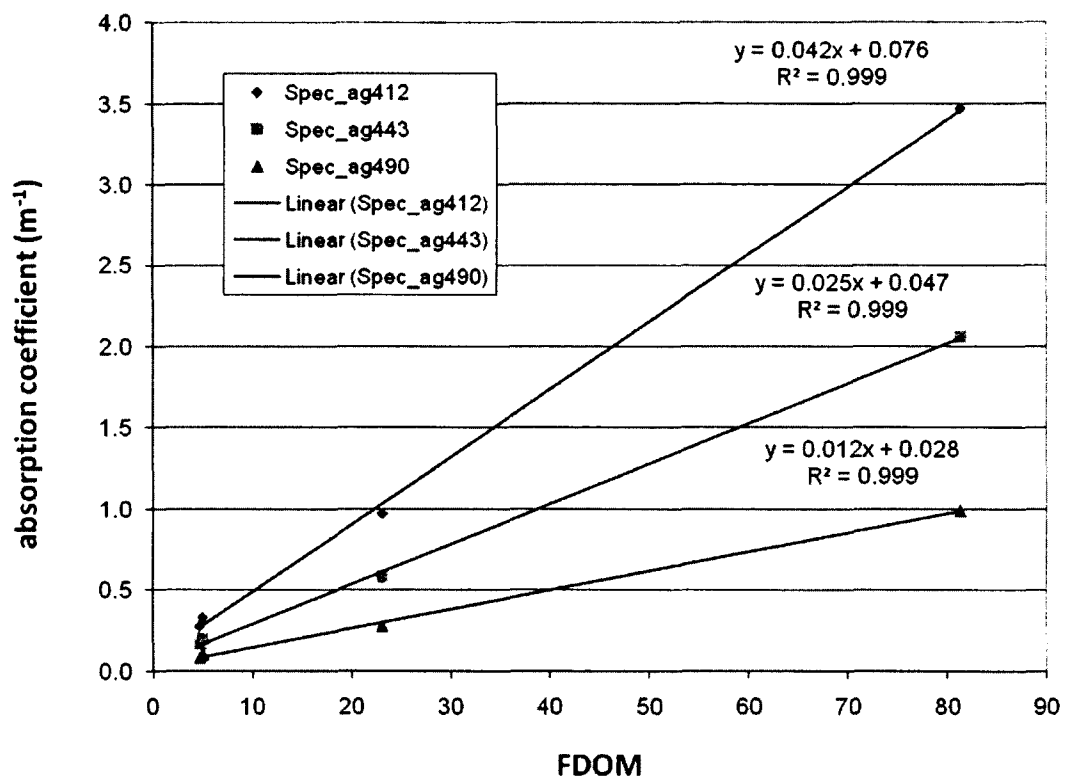


Figure 2. Graph for February 17, 2005 cruise showing spec ag (light absorption of CDOM) vs. FDOM at 3 different wavelengths: 412, 443, and 490 nm. The three different lines are related to each other by the value of the spectral slope S.

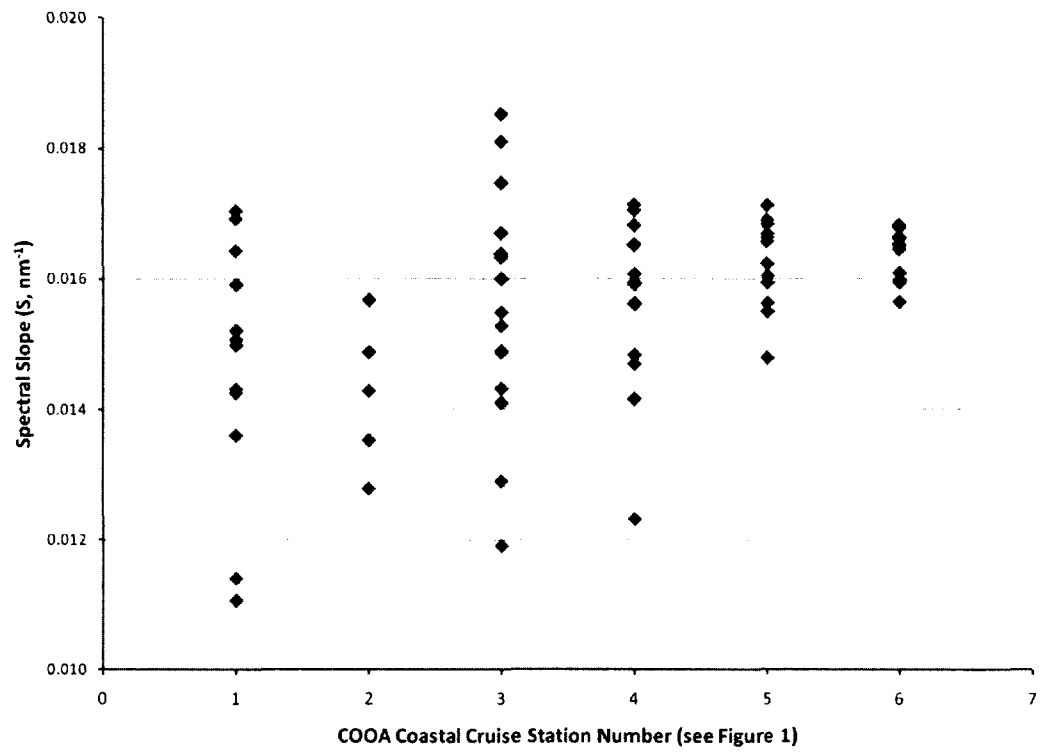


Figure 3. Spectral slopes (S in equation 1.1) for $ag(\lambda)$ data at each COOA Coastal Transect station.

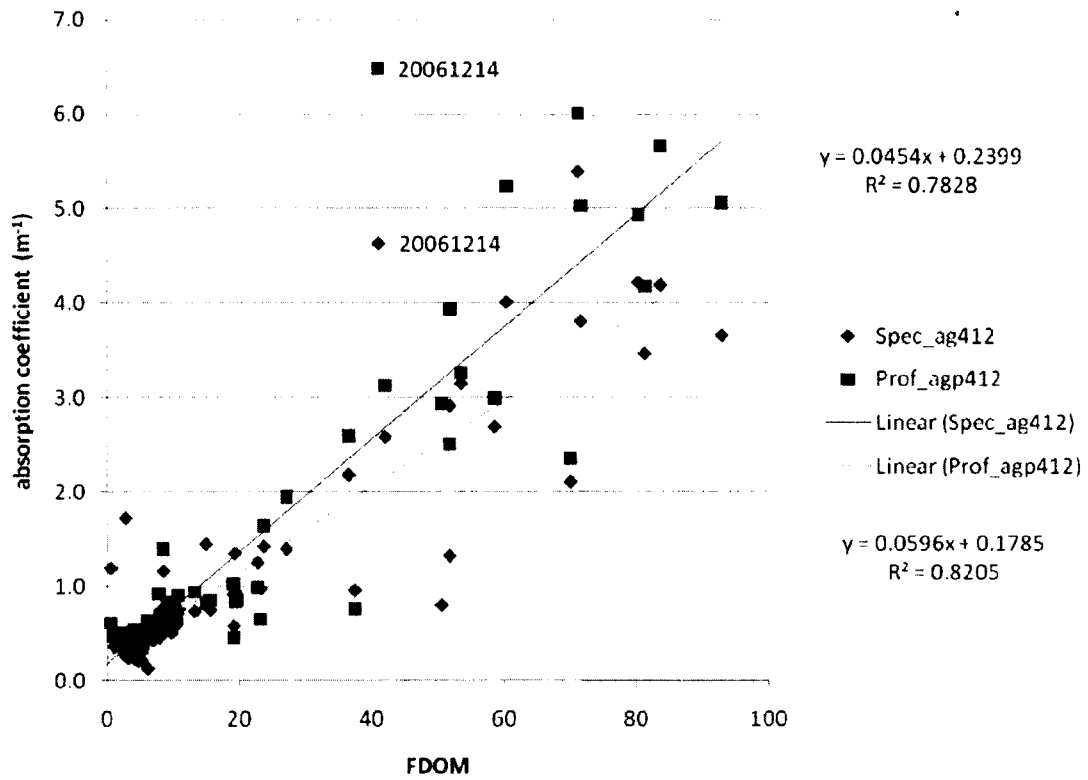


Figure 4. Absorption coefficients, ag412 (blue) and agp412 (red), plotted against FDOM for all stations in the database. Regression equations are shown for ag412 (top right) and agp412 (bottom right). Large departures from these regression curves (e.g., data for CT cruise 20061214) indicated the need to derive regressions for each individual cruise.

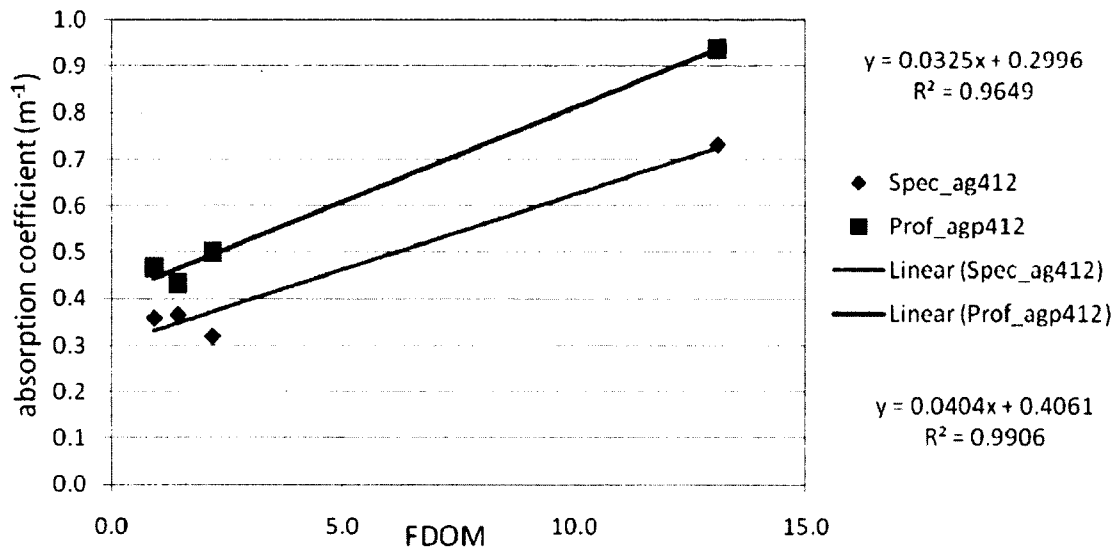


Figure 5. Calibration regression data for September 24, 2004 cruise. Flow-through FDOM (ppb) is on the horizontal axis. For every figure the spec linear regression equation is on the top right, while the bottom right linear regression equation is for the profiler.

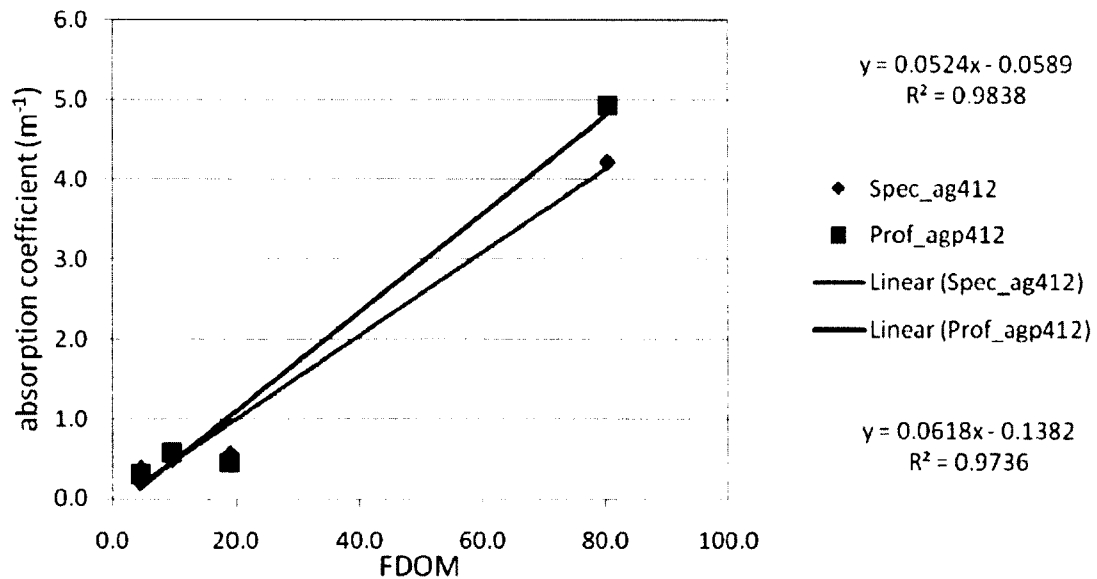


Figure 6. Calibration data for November 4, 2004.

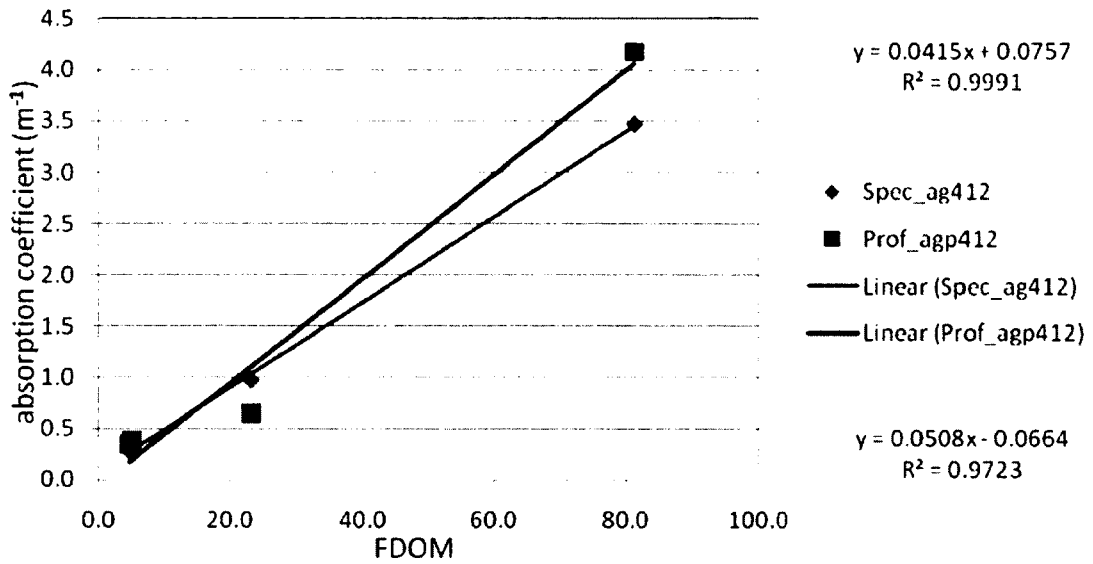


Figure 7. Calibration data for February 17, 2005.

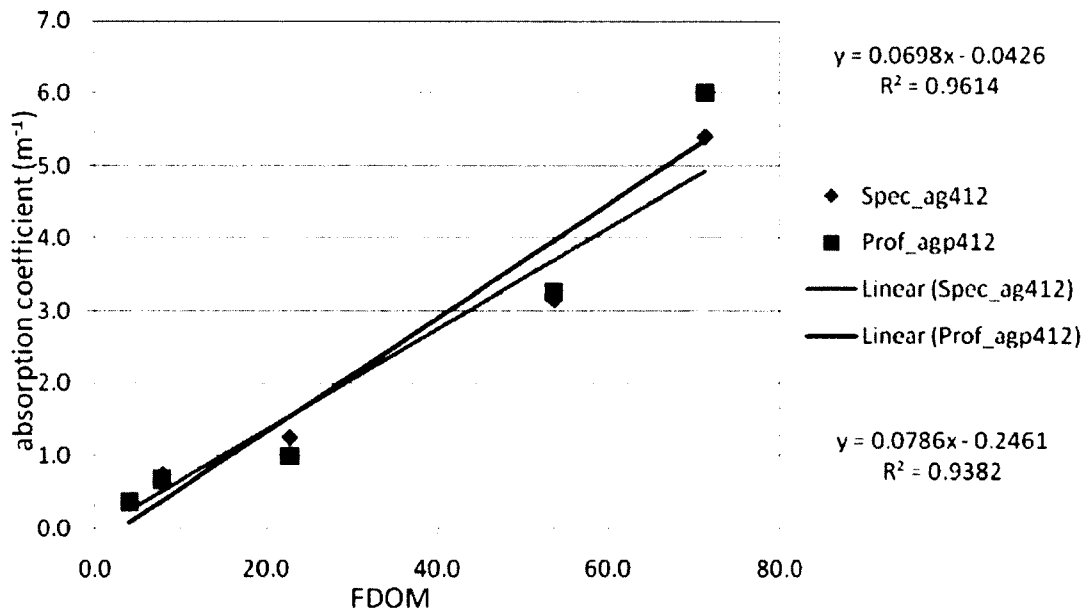


Figure 8. Calibration data for June 29, 2005.

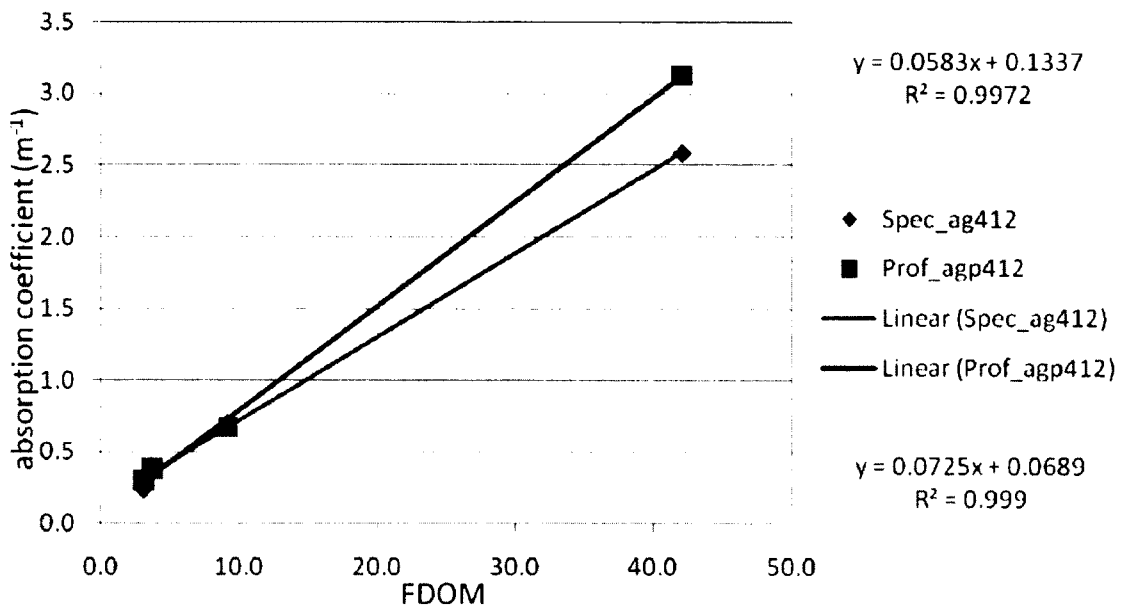


Figure 9. Calibration data for August 17, 2005.

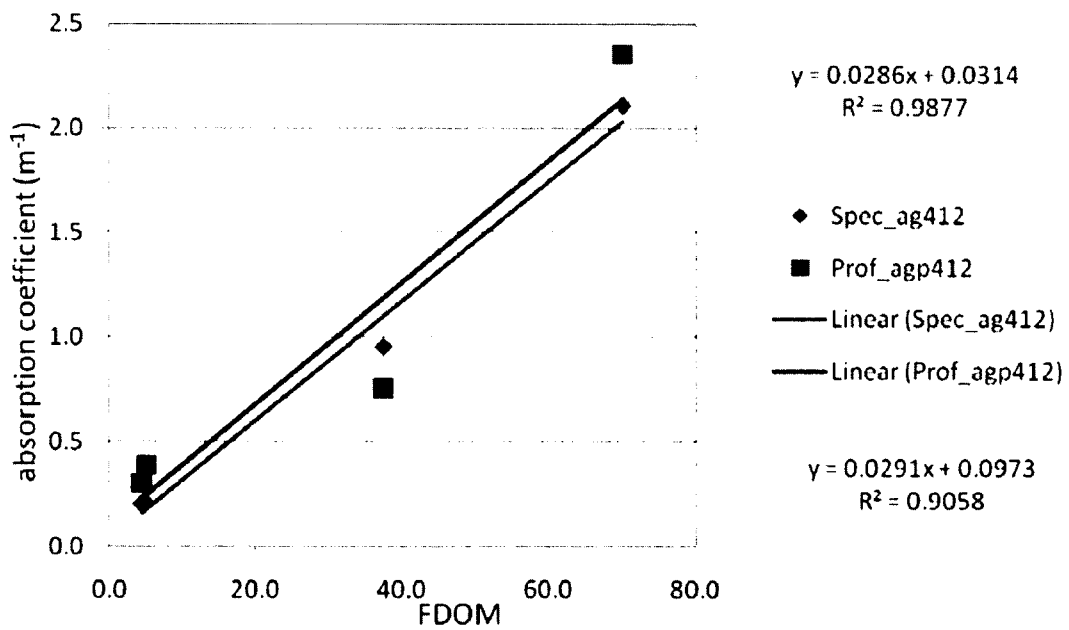


Figure 10. Calibration data for February 22, 2006.

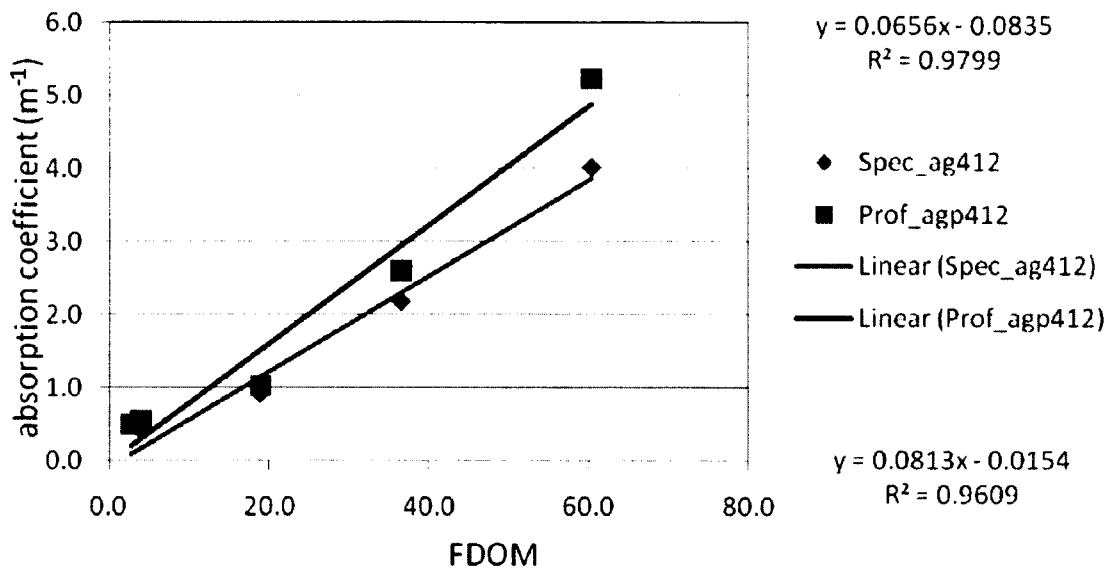


Figure 11. Calibration data for July 19, 2006.

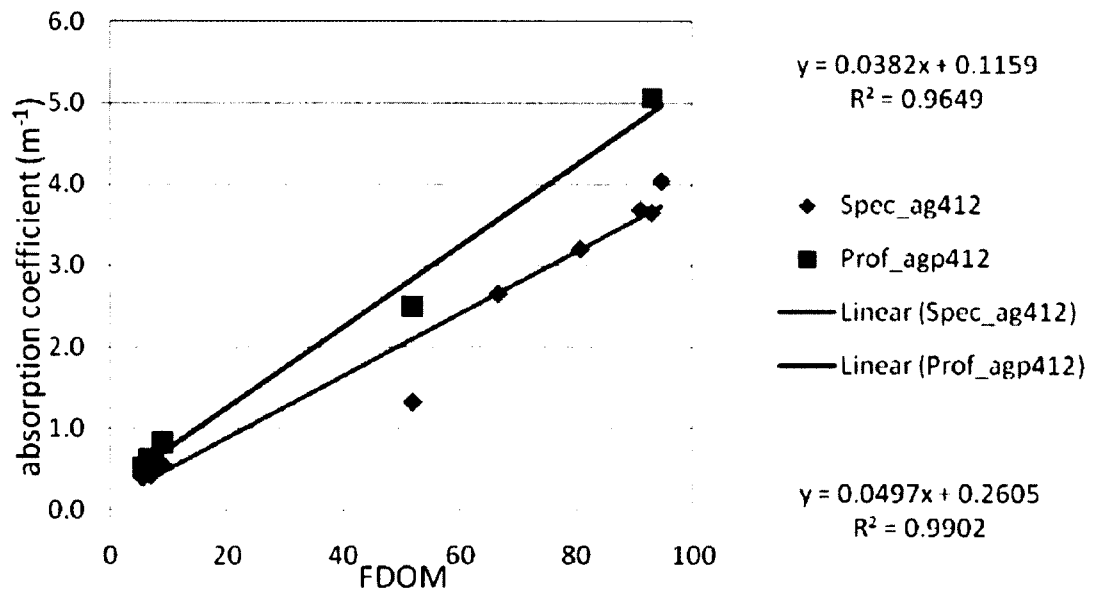


Figure 12. Calibration data for September 15, 2006.

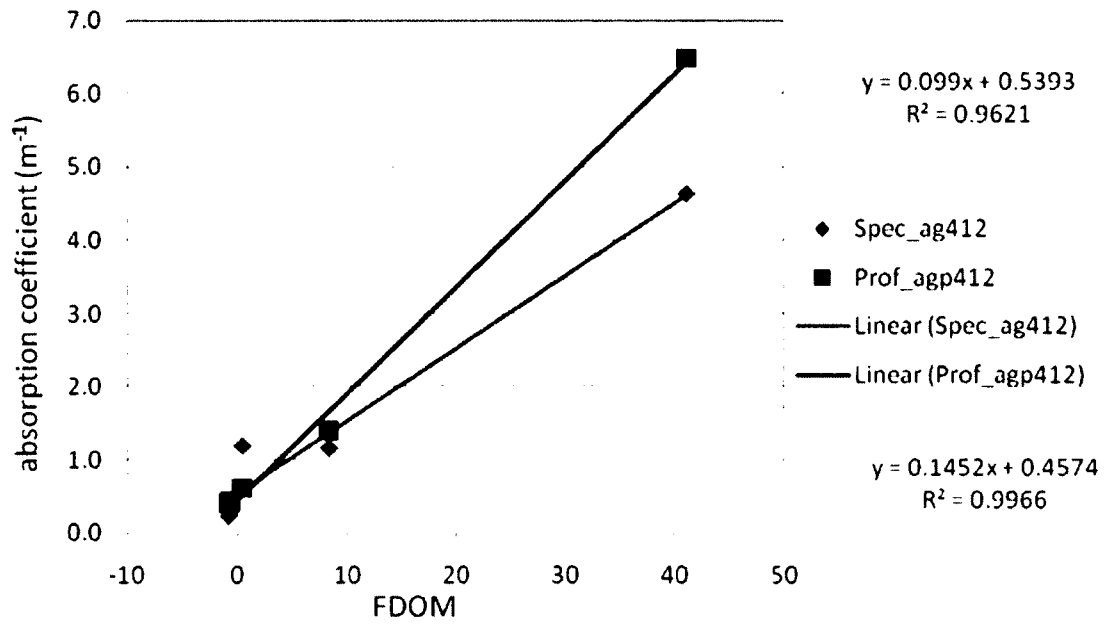


Figure 13. Calibration data for December 14, 2006.

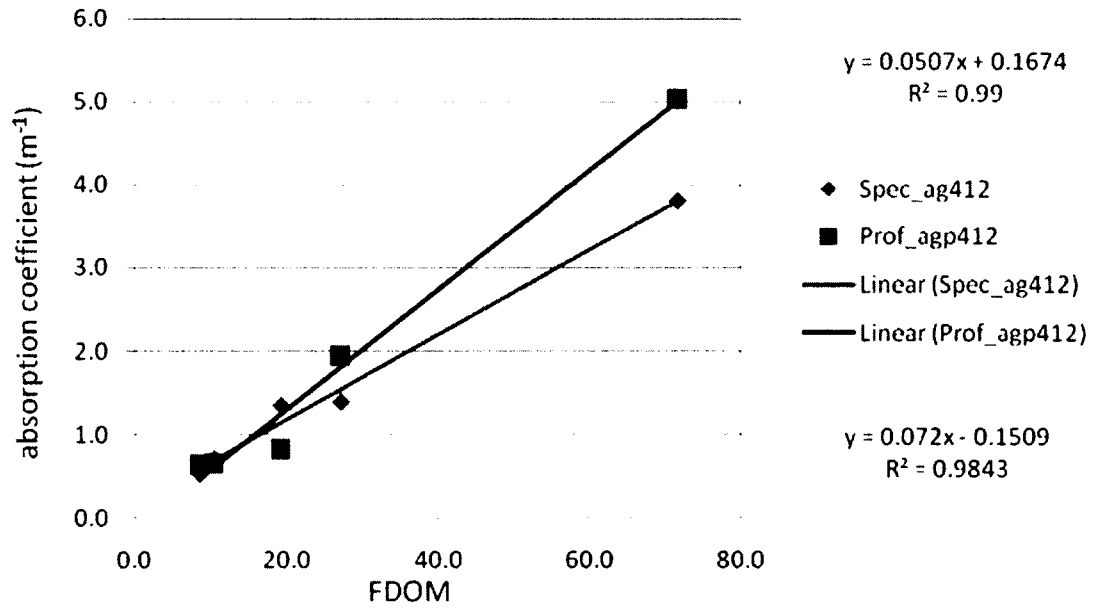


Figure 14. Calibration data for May 7, 2007.

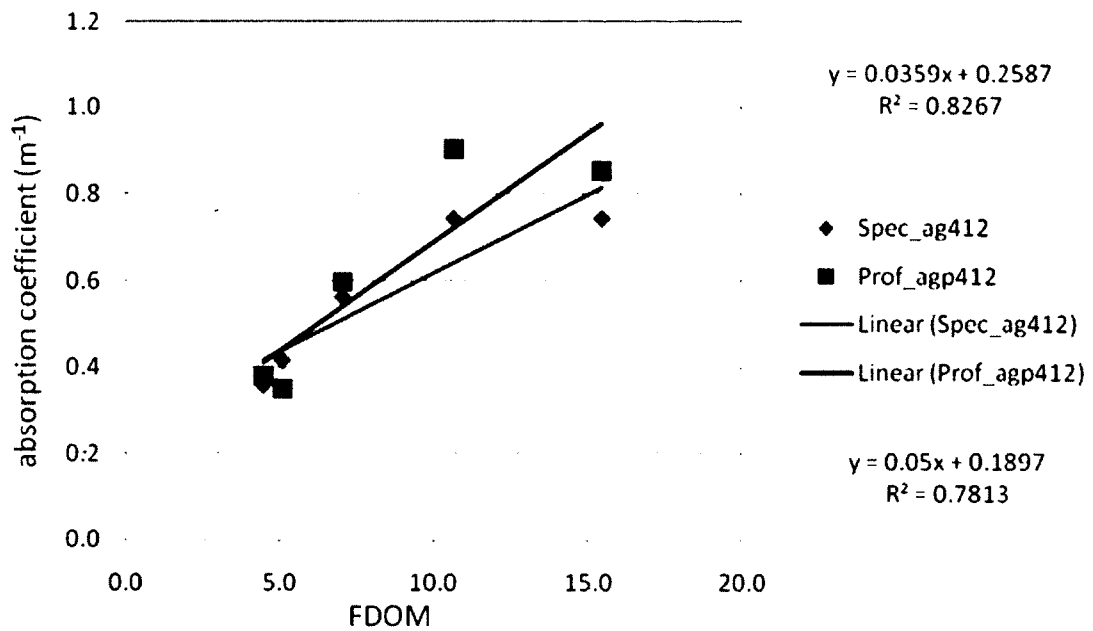


Figure 15. Calibration data for June 19, 2007.

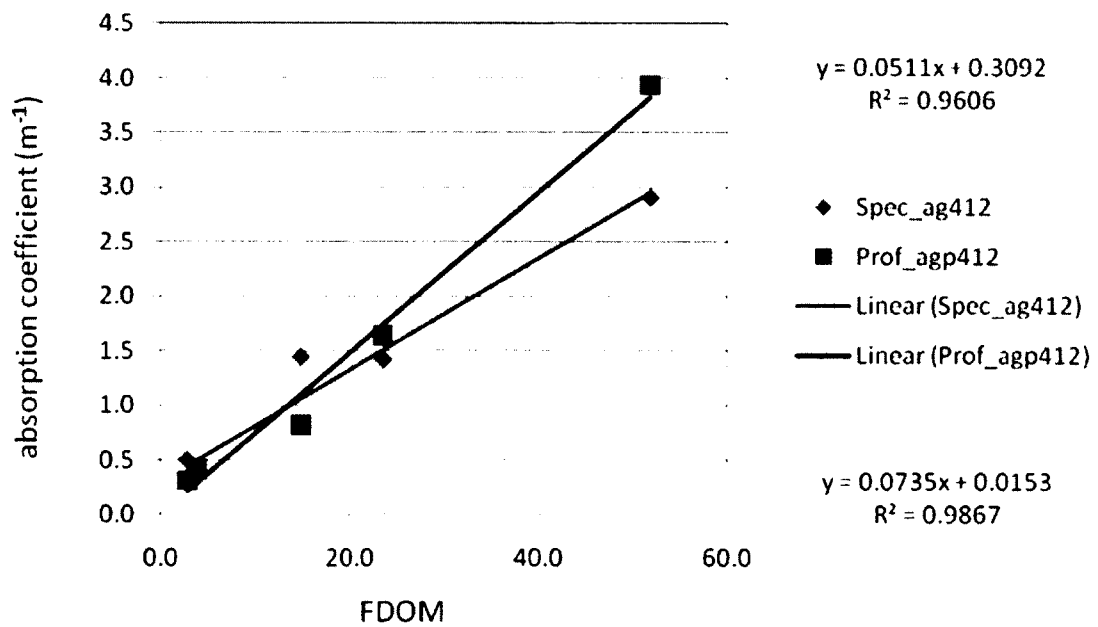


Figure 16. Calibration data for August 21, 2007.

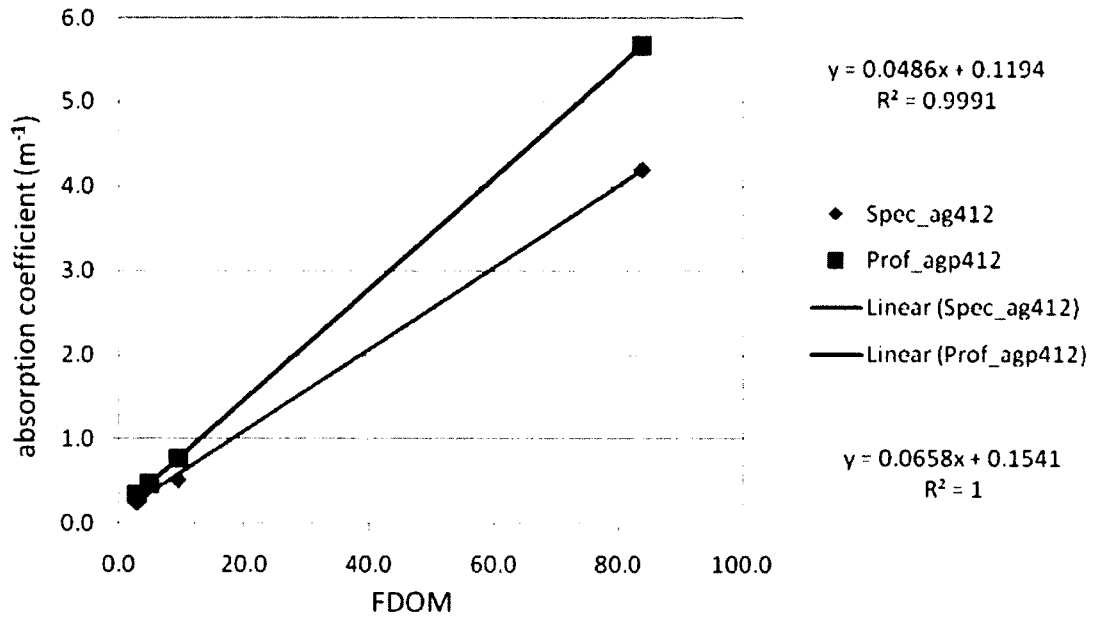


Figure 17. Calibration data for November 13, 2007.

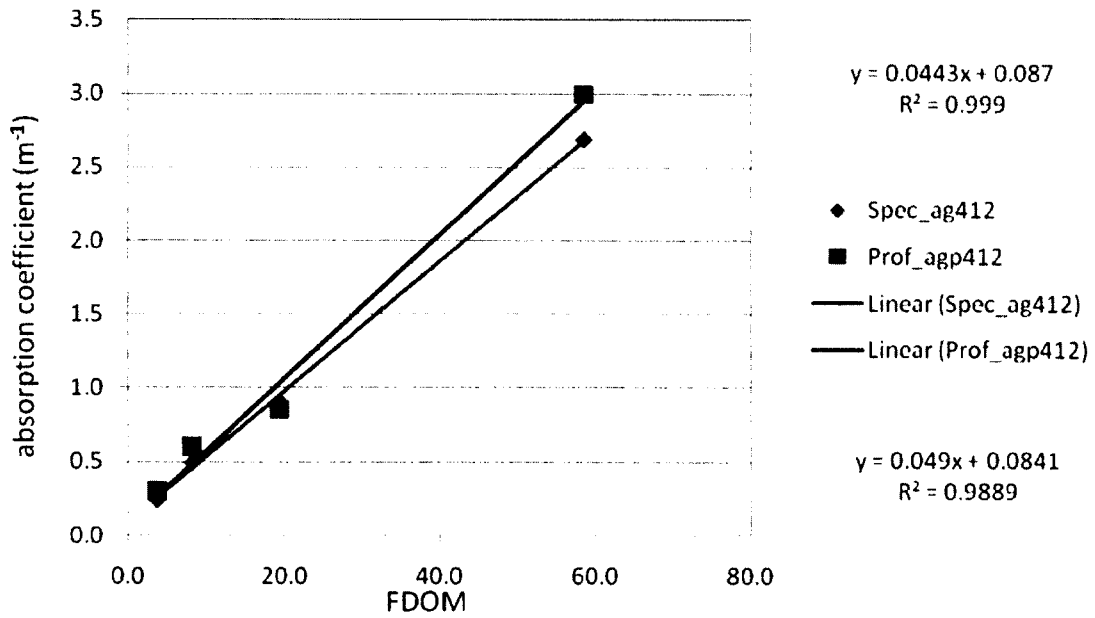


Figure 18. Calibration data for January 16, 2008.

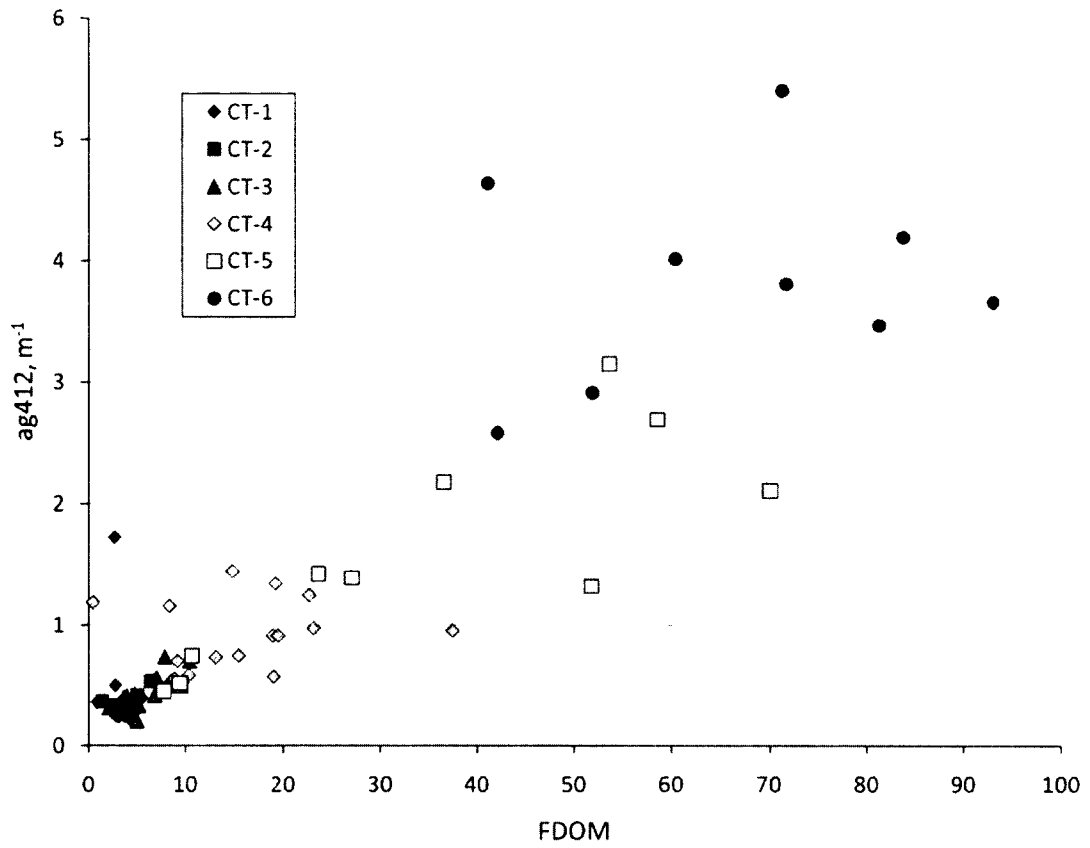


Figure 19. Spectrophotometer ag412 vs. FDOM color-coded by Coastal Transect station number. Stations 4, 5 and 6 show the influence of freshwater from the Kennebec River Estuary.

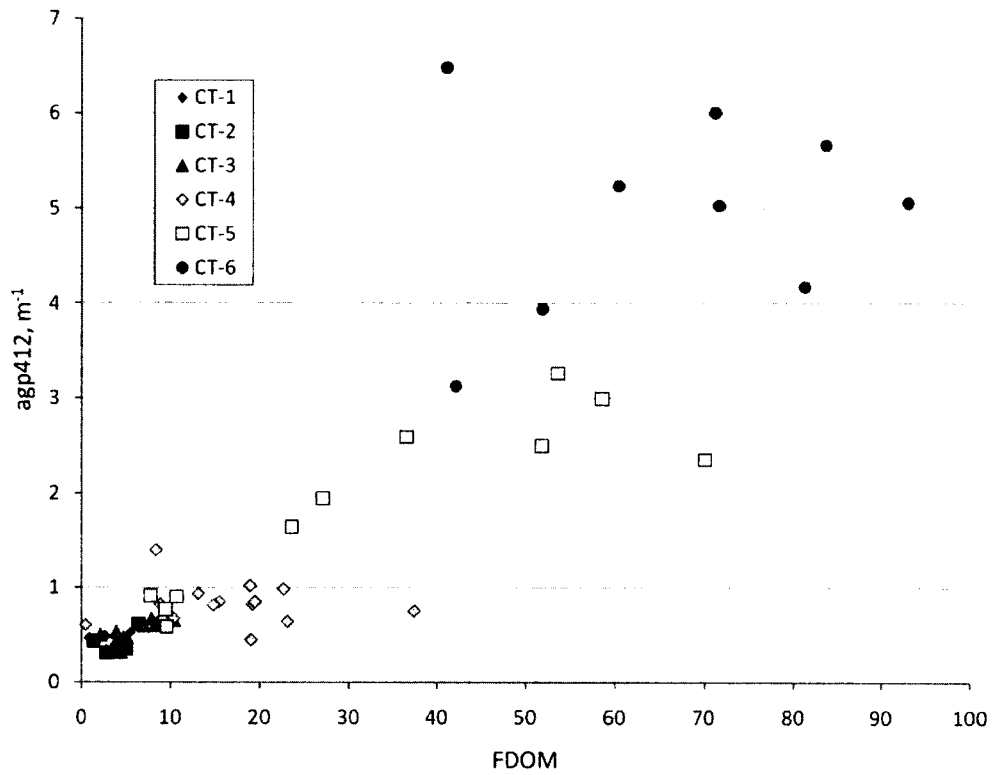


Figure 20. Profiler agp412 vs. FDOM color-coded by Coastal Transect station number.

CHAPTER 3

INVESTIGATING CDOM AS A TRACER OF FRESHWATER

This chapter explores the variability of CDOM in relation to salinity in the Kennebec Estuary, and the use of CDOM as a freshwater tracer. Specifically, this research investigates whether the variability of the CDOM absorption coefficient exhibits any predictable trends or patterns related to discharge. To obtain the results for this chapter, the continuous underway FDOM was converted to CDOM absorption (ag412) using the “calibration curves” derived in Chapter 2 (Table 1). Use of the underway data makes possible the examination of the variability of CDOM absorption with respect to salinity, which was also measured continuously while underway.

This research searches for a predictable relationship between salinity and CDOM absorption, such that CDOM could act as a freshwater tracer along this cruise track. In this context, CDOM absorption is considered a surrogate for the mass concentration of CDOM. A simple linear relationship between CDOM absorption and salinity would indicate that CDOM behaves conservatively within the river, ranging between high values upstream and low values offshore. The relationship may be useful in remote sensing of CDOM as a surrogate for salinity provided that its slope and intercept are

predictable. Thus, variability in the relationship was examined in relation to river discharge, season, and other factors. A predictable relationship between discharge and CDOM absorption would have important applications to remote sensing because then CDOM absorption levels observed from space or aircraft could quantify the spatial extent of freshwater in a given area (Salisbury 2008, 2011).

In the previous chapter, it was shown that CDOM levels at the estuarine stations (stations 5 and 6) varied considerably between cruises. In this chapter, hypotheses are considered to explain that variability in terms of the relationship between river discharge and CDOM levels. These hypotheses would predict either a direct or inverse relationship, depending upon the scenario. A direct relationship, in which high discharge rates result in high CDOM, occurs when, for example, a river swollen by heavy rains washes a lot of CDOM from the soil and transports it out to sea. On the other hand, high discharge might result in a low CDOM absorption when, for example, stormflow dilutes river water and decreases the CDOM absorption per unit volume of the river. As a result, high discharge rates yield low CDOM absorption, and low discharge rates yield high CDOM absorption.

Another hypothesis, herein called the residence time hypothesis, describes an inverse relationship between discharge and CDOM. According to the residence time hypothesis, higher discharge levels flush the river, decrease the residence time of CDOM in the stream, and result in a lack of CDOM accumulation. Lower discharge rates allow for CDOM buildup, and increase the residence time of CDOM. In this scenario, as CDOM

builds up in the stream, it would no longer vary conservatively with freshwater, but would exhibit nonlinear behavior with salinity. A more linear relationship between CDOM absorption and salinity would exist when the residence time is shorter.

Seasonal variation in the amount of CDOM entering the river might also be predictable. It is expected that higher levels would exist in the late fall and winter after the fallen leaves have begun to decompose. However, CDOM exported from salt marshes is known to peak in late summer (Gardner et al. 2005). Thus, a seasonal pattern was also considered.

Data and Methods

The **flow-through salinity and FDOM data** for the 14 cruises were retrieved from the UNH COOA Coastal Transect (CT) cruise datasets. The FDOM data were converted to CDOM absorption coefficients (ag412) using the linear equations of the “calibration curves” (Table 1). Then graphs of ag412 vs. salinity were plotted for each of the 14 cruises.

Discharge data were obtained from USGS Real-Time Water Data files of the Kennebec River at North Sidney, Maine, and the Androscoggin River near Auburn, Maine (<http://waterdata.usgs.gov/nwis/rt>). The USGS files are based on measurements of discharge rates at these and other rivers in the U.S. every 15 minutes for every day of the year. Instantaneous discharge (Q) is measured in cubic feet per second (ft³/s). The site also provides mean daily rates for each day.

Daily discharge rates were extracted from the USGS files for the 14 cruise dates. The two separate daily discharge rates of the Kennebec River and the Androscoggin River were summed and entered as one value representing the daily discharge rate of the Kennebec-Androscoggin River System (Q_{daily}). Cumulative discharge rates for each cruise were calculated by summing daily discharge values for the day of the cruise and the 7 days previous to the cruise, for a total of 8 days. Then the 8-day average discharge rates (Q_{avg}) were calculated by dividing the cumulative discharge rates by 8. Finally, a discharge difference (ΔQ) was calculated by subtracting the daily discharge rate from the average discharge rate. Table 4 lists the 14 cruise dates and daily, cumulative, and average discharge rates, as well as the corresponding discharge differences (ΔQ).

To characterize the variability of CDOM vs. salinity curves from different cruises, $ag412$ values were extracted at three points along each curve: at **zero salinity**, **maximum salinity**, and at a **salinity of 15 PSU**. The salinity of 15 PSU was chosen because all of the cruises have data for this salinity. The $ag412$ value at zero salinity was estimated in cases where the cruises never reached a station with zero salinity. The height of the curve at $S=15$ was compared to the CDOM absorption value on a line drawn between the zero and maximum salinity points to ascertain whether CDOM levels are above or below the conservative mixing line. A CDOM source raises CDOM absorption levels above the conservative line, whereas a CDOM sink results in lower CDOM values below this line.

The CDOM absorption vs. salinity graphs demonstrate **nonlinearity**, which contributes to the complexity of CDOM variability in relation to salinity. A second-order quadratic equation was fitted to each individual graph. The quadratic coefficient describes the degree of the curvature, and the intercept of the curve was used to estimate the zero salinity value. The CDOM difference, ΔCDOM , between the curve height and the conservative line at 15 PSU was derived as a measure of the nonconservative behavior of CDOM.

Results

The relationship between CDOM absorption and salinity, as depicted in figures 21-23, was highly variable over the course of any given year and also over a period of several years. Offshore values were relatively stable whereas the estuarine, low-salinity CDOM values were the source of the variability with values ranging between 2 m^{-1} and 6 m^{-1} .

The box on each figure contains the daily and cumulative (8-day) discharge rates corresponding to the cruise dates on the adjacent legend. (Please refer to Table 4 for a complete listing of the discharge rates for the 14 cruises). Each cruise is different, and no pattern emerges to explain the variance. The date with the highest discharge was May 7, 2007, and yet the CDOM curve for that day is about midway between the highest and lowest curves for that year (Figure 23).

The large square symbols on each curve in figures 21-23 indicate the locations of stations 4, 5, and 6. The salinity at these stations varied from cruise to cruise (Table 5)

and reflects variations in the tidal stage and the spatial extent of the river plume. The effects of the river plume were often first apparent at station 4 near Sequin Island, and in some cases, there was a lower salinity at that station than at station 5 which was located at the entrance to the Kennebec River Estuary.

CDOM (ag412) values associated with the 14 cruises at zero salinity, maximum salinity, and salinity = 15 PSU are listed in Table 6. Also listed in this table is Δ CDOM, the difference between the measured CDOM absorption and the linear estimate of CDOM absorption at salinity=15 PSU. A schematic illustrating the concept of Δ CDOM is presented in figure 24.

A plot of Δ CDOM vs. Julian day (Figure 25) exhibits slightly higher Δ CDOM in the summer months compared with other times of year, suggesting a tendency for CDOM to accumulate in the river in summer. Δ CDOM vs. Q_{daily} , Δ CDOM vs. Q_{avg} , and Δ CDOM vs. ΔQ are shown in figures 26-28, respectively. The day with the highest values of Q_{daily} , Q_{avg} , and ΔQ , May 7, 2007, had a relatively low value of Δ CDOM, which would be consistent with the residence time hypothesis. That is, the low Δ CDOM indicates a more linear curve and thus conservative behavior of the CDOM that is being flushed through the estuary. On the other hand, days with the highest Δ CDOM occurred when the discharge rates were relatively low ($\leq 10000 \text{ ft}^3/\text{s}$). These results are not definitive, but only suggestive that the residence time hypothesis is supported.

Discussion

From year to year and from season to season, the most remarkable observation is the high CDOM variability in the Kennebec Estuary. CDOM absorption varies significantly each year and each season for the 14 cruises from 2004-2008. In addition, each cruise displays different CDOM absorption results across a similar salinity range. Why are CDOM levels so variable? The CDOM variability is dramatic, yet it appears to have no predictability or explanation given the observations presented here.

The relationship between **river discharge and CDOM** displays no obvious trend, and therefore does not adequately explain CDOM variability (Figures 21-23). If discharge and CDOM absorption reflected one of the discharge rate hypotheses, discharge rates would be either directly or inversely correlated to CDOM absorption. Instead, CDOM absorption neither increases nor decreases with increasing discharge, but appears random with respect to discharge rates. However, there is some indication that high discharge results in a more conservative behavior of CDOM (linear, low Δ CDOM), which would be suggestive of the residence time hypothesis.

The **Δ CDOM vs. Julian day** graph reveals a tendency towards slightly higher CDOM accumulation in the summer as opposed to the winter (Figure 25). The CDOM difference (Δ CDOM) essentially indicates how much CDOM has accumulated or entered the water laterally as compared with CDOM transported conservatively from upstream sources. The fact that Δ CDOM is always at least slightly positive indicates that CDOM accumulation is continually present at any time during the year for all 14 cruises. Most

notably, the graph shows slightly elevated ΔCDOM between days 175-250 (June-September), and slightly lower values on days 0-60 (January-February). This difference could signal the addition of a CDOM source in the summertime. According to Gardner et al. (2005), the growth of salt marshes, which are a source of CDOM in estuaries, peaks in late summer at the end of the growing season. Salt marshes fringe the Kennebec Estuary in several areas, so it is possible that organic matter degradation in these marshes adds CDOM to the water and causes increases in CDOM in the Kennebec Estuary during the summer months.

It is well known that salt marshes show seasonal variability in their contribution of CDOM and DOC to estuaries and ultimately the ocean (Wang et al. 2007). However, some of the CDOM variability observed in the data could possibly result from the influence of the tidal cycle in the Kennebec Estuary. Although this research did not examine tidal phases for any of the cruises in the Kennebec Estuary, speculation is that the point at which salinity = 15 relative to the location of the salt marshes would have moved with the tides. As a result, the changing tides could have been a factor in causing ΔCDOM to fluctuate. Clark et al. (2008) and Tzortziou et al. (2008) observed significantly higher CDOM absorption levels during ebb tides as compared with flood tides, which dilute CDOM. Flood tides or high tides would shift the salinity = 15 point upstream. So, the phase of the tide when CDOM absorption was measured could have influenced the impact of salt marshes on the observed CDOM accumulation and ΔCDOM variability in the Kennebec Estuary.

The ΔCDOM vs. discharge graphs do not present distinct patterns of how the discharge rate affects CDOM variability, but they do permit speculation concerning potential causes of ΔCDOM variance (Figures 26-28). All of the graphs show positive ΔCDOM values, indicating the presence of at least one source adding CDOM to the river as the water moves downstream. The most salient characteristic of the graphs are the two outliers that depart from the cluster of data points in the lower left quadrant. These two outlying points are the only points that clearly support the residence time hypothesis. One point, May 7, 2007, demonstrates the residence time hypothesis with the highest values of Q_{daily} , Q_{avg} , and ΔQ , and a relatively low ΔCDOM . High discharge rates flush the river and reduce CDOM accumulation. The other data point, June 29, 2005, pairs relatively low values of Q_{daily} , Q_{avg} , and ΔQ with a very high ΔCDOM . Low discharge rates allow for CDOM buildup. The other data points exhibit this pattern slightly, with relatively high discharge rates corresponding to lower CDOM accumulation, and low discharge rates correlating with higher CDOM accumulation. As evidenced in these graphs by the data distribution, discharge rate could play a role in controlling the ΔCDOM variability, or the variability of CDOM accumulation in Kennebec Estuary.

The discharge difference, ΔQ , which is the difference between the average and daily discharge rates, provides a clue to weather conditions driving discharge rates, which in turn might affect CDOM variability (Figure 28). For instance, a major storm event during the week before a cruise could cause the average discharge rate to soar, resulting in a large positive discharge difference between the average rate and that on

the day of the cruise. However, this parameter does not provide additional insight concerning the relationship between the Δ CDOM and the discharge.

The **convex curvature** of the graphs in figures 21-23 indicates a possible **CDOM source or sources** contributing to CDOM variability as the water moves downstream, but ascertaining the exact origins or causes of the CDOM increase proves challenging due to a number of possible influences. For one, CDOM produced in salt marshes or coastal wetlands could enter the Kennebec Estuary and increase CDOM in the water column (Chen and Gardner 2004; Gardner et al. 2005). Secondly, according to the residence time hypothesis, an increased residence time, such as in response to a low discharge rate, could allow for CDOM to accumulate in the water due to *in situ* biological production by phytoplankton (Chen and Gardner 2004; Gardner et al. 2005). Thirdly, temporal variations in river input, such as a surge in the river in the days following a storm or heavy rains, could wash a large amount of CDOM from the soil and suddenly raise CDOM levels in the estuary (Gardner et al. 2005). Finally, anthropogenic inputs, such as pollution from factories adjacent to the water, could deposit additional CDOM into the water (Salisbury et al. 2008). The physical complexities of the watershed complicate the detection of the exact CDOM sources.

Conclusions

In the introduction to this chapter, hypotheses were described that would predict either a direct or inverse relationship between CDOM and discharge. The fact that neither of these was found to be the trend in the Coastal Transect cruise data

suggests that the explanation is complex. It is concluded that both hypotheses operate at different times or at the same time but with different strengths. The two are not mutually exclusive. In other words, high CDOM entering the river after a storm would be associated with high discharge but it might be diluted by rainwater. A long residence time during periods of low discharge would be associated with increased curvature indicating an accumulation of CDOM in the river relative to that entering upstream, but the source waters might be low in CDOM since the runoff is low.

The data suggest that the residence time provides a plausible explanation for Δ CDOM variability in the Kennebec Estuary. The perpetual positive Δ CDOM values indicate a CDOM source or sources adding CDOM to the water as it moves downstream. Salt marshes fringing the river in several areas are a possible CDOM source. Elevated summer Δ CDOM levels, signaling an increase in CDOM accumulation in the river, could result from the growth of salt marshes peaking in late summer.

Table 4. Cruise date with corresponding Julian day, daily discharge, cumulative discharge, average discharge, and discharge difference in ft³/s for all 14 cruises.

Cruise Date	Q _{daily}	Q _{cumul}	Q _{avg}	ΔQ	Julian Day
9/24/2004	10680	86710	10839	159	268
11/4/2004	6690	52060	6508	-182	309
2/17/2005	12620	84160	10520	-2100	48
6/29/2005	11020	132410	16551	5531	180
8/17/2005	5270	42080	5260	-10	229
2/22/2006	17090	146040	18255	1165	53
7/19/2006	9600	81800	10225	625	200
9/15/2006	10190	77890	9736	-454	258
12/14/2006	16130	128630	16079	-51	348
5/7/2007	37800	408200	51025	13225	127
6/19/2007	7090	80400	10050	2960	170
8/21/2007	4670	48030	6004	1334	233
11/13/2007	14190	165900	20738	6548	317
1/16/2008	18910	197690	24711	5801	16

Table 5. Salinity levels at stations 4, 5, and 6 for each of the 14 cruises. Salinity values are in practical salinity units (PSU). Note that station 6 was not reached on 9/24/2004, and water samples were not collected at station 5. All other cruises reached station 6 although water samples were not collected at station 6 on every cruise (see Table 1).

Cruise Date	Station 4	Station 5	Station 6
9/24/2004	27.3	21.7	----
11/4/2004	26.1	30.1	1.1
2/17/2005	25.3	15.1	0.7
6/29/2005	25.0	14.5	0.7
8/17/2005	28.0	25.7	11.6
2/22/2006	23.5	14.8	1.6
7/19/2006	24.4	17.3	2.2
9/15/2006	27.6	18.4	3.0
12/14/2006	26.2	16.1	0.7
5/7/2007	25.9	21.8	0.5
6/19/2007	25.8	28.6	8.9
8/21/2007	26.0	22.0	6.0
11/13/2007	30.0	30.4	11.4
1/16/2008	26.7	12.8	0.4

Table 6. Cruise date with corresponding Julian day, ag412 at salinity=0, ag412 at maximum salinity, maximum salinity (PSU), ag412 at salinity=15 PSU, and Δ CDOM for all 14 cruises.

Cruise Date	ag412 @sal=0	ag412 @max sal	Max Sal	ag412 @sal=15	Δ CDOM	Julian Day
9/24/2004	3.085	0.313	31.5	2.075	0.309	268
11/4/2004	4.310	0.153	32.1	2.612	0.244	309
2/17/2005	3.555	0.259	31.8	2.276	0.276	48
6/29/2005	4.515	0.260	29.9	3.662	1.282	180
8/17/2005	3.209	0.267	31.1	2.290	0.499	229
2/22/2006	3.378	0.154	32.6	2.010	0.118	53
7/19/2006	3.946	0.042	30.9	2.611	0.563	200
9/15/2006	3.858	0.344	31.2	2.523	0.351	258
12/14/2006	4.738	0.451	32.6	3.033	0.267	348
5/7/2007	3.853	0.537	29.6	2.467	0.297	127
6/19/2007	2.623	0.344	31.3	1.812	0.281	170
8/21/2007	3.212	0.430	31.4	2.229	0.344	233
11/13/2007	5.996	0.243	32.1	3.657	0.347	317
1/16/2008	3.952	0.224	32.5	2.387	0.155	16

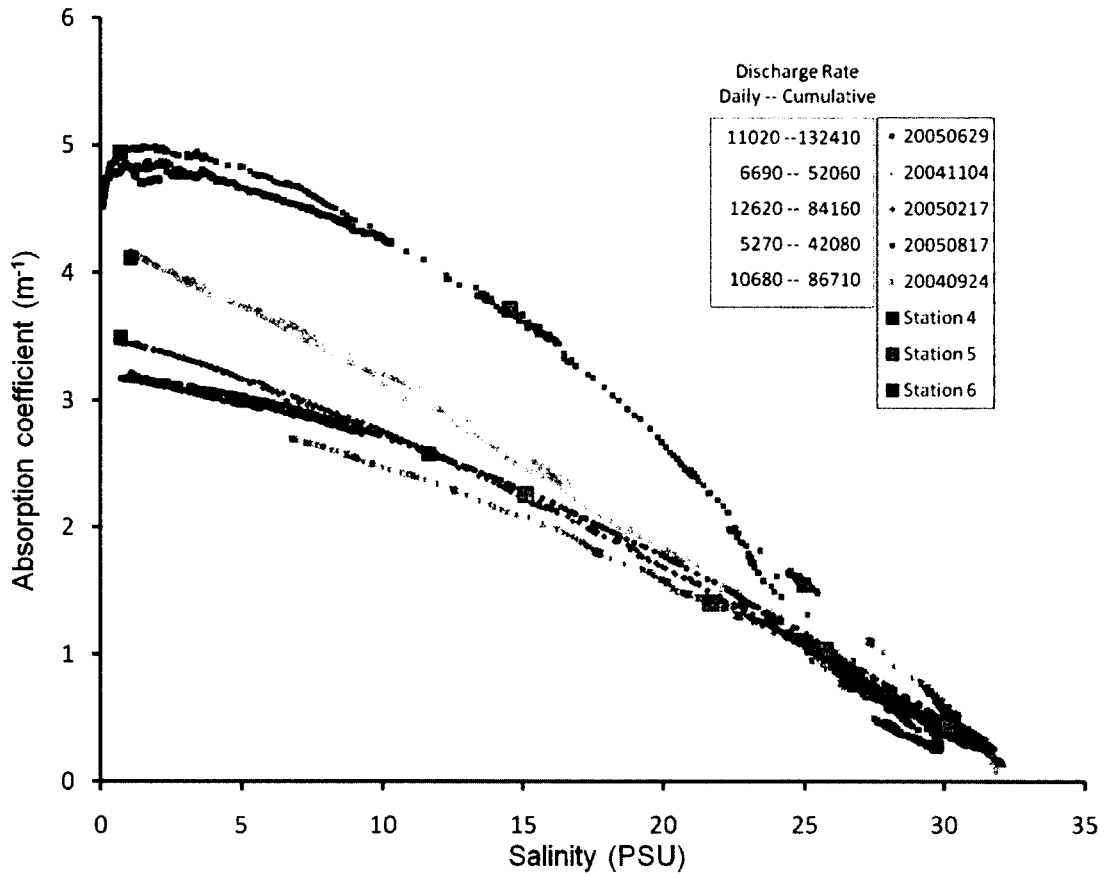


Figure 21. CDOM absorption coefficient vs. salinity for COOA Coastal Transect cruises in 2004 and 2005. Daily and 8-day cumulative discharge rates are shown next to the figure legend. The locations of stations 4 (blue), 5 (green) and 6 (red) are indicated by large square symbols.

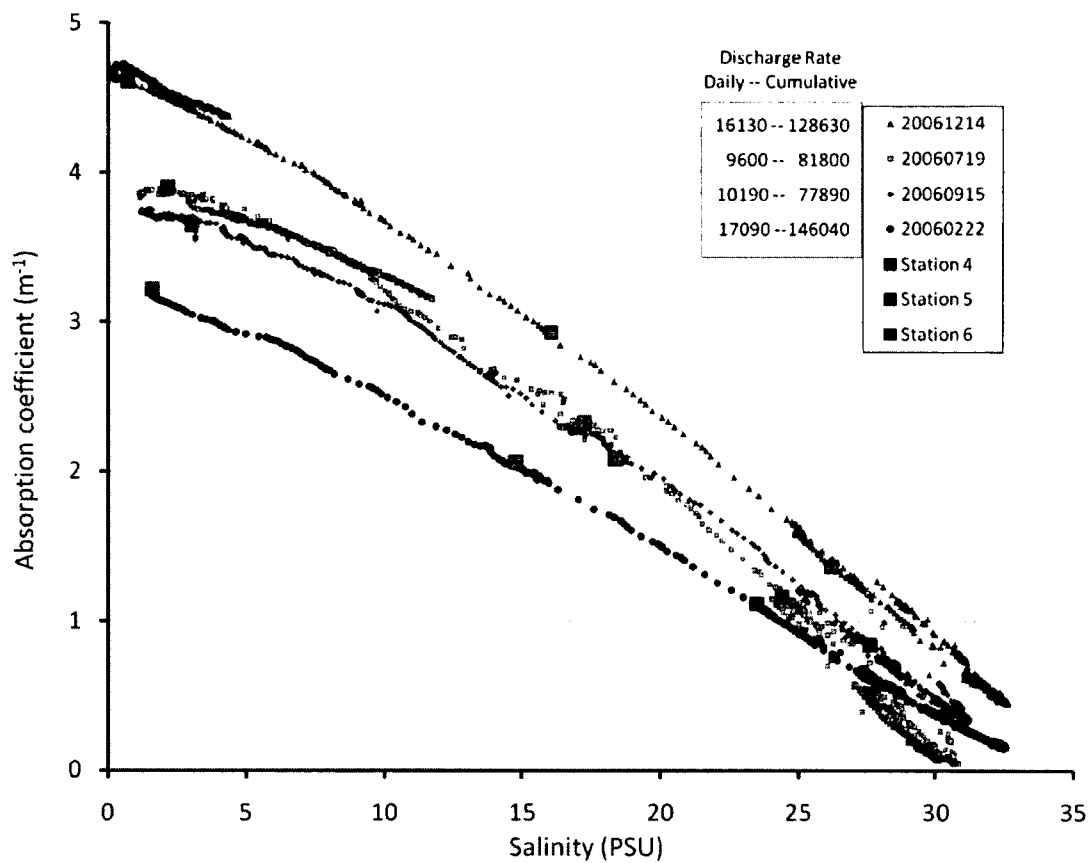


Figure 22. CDOM absorption coefficient vs. salinity for COOA Coastal Transect cruises in 2006. Daily and 8-day cumulative discharge rates are shown next to the figure legend. The locations of stations 4 (blue), 5 (green) and 6 (red) are indicated by large square symbols.

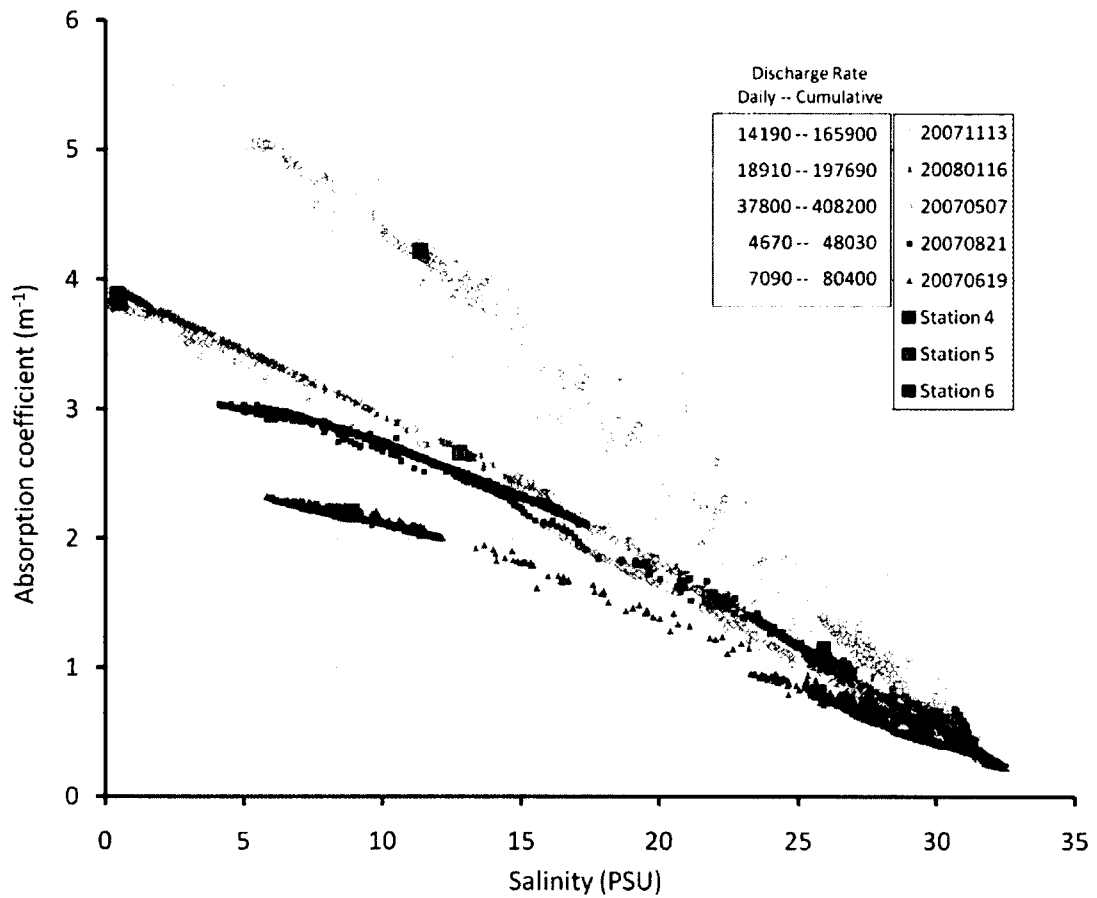


Figure 23. CDOM absorption coefficient vs. salinity for COOA Coastal Transect cruises in 2007 and 2008. The locations of stations 4 (blue), 5 (green) and 6 (red) are indicated by large square symbols.

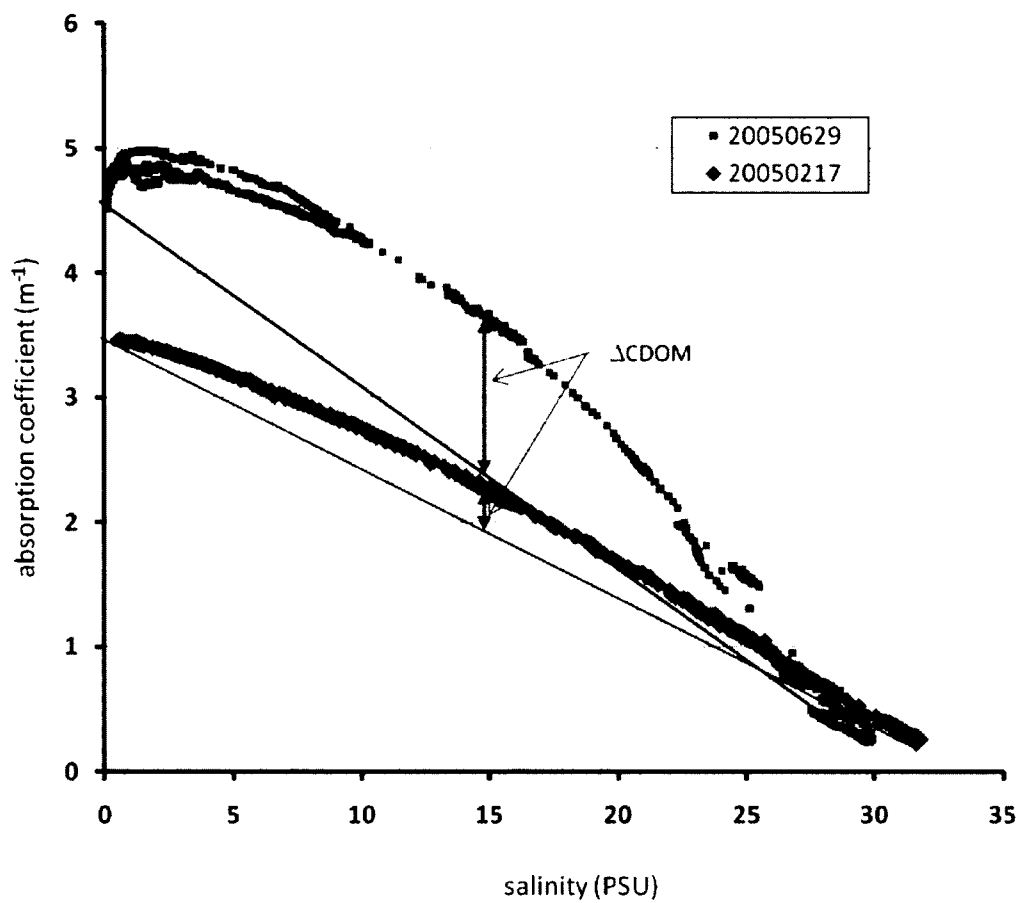


Figure 24. Schematic illustrating ΔCDOM representing departure from a conservative mixing line.

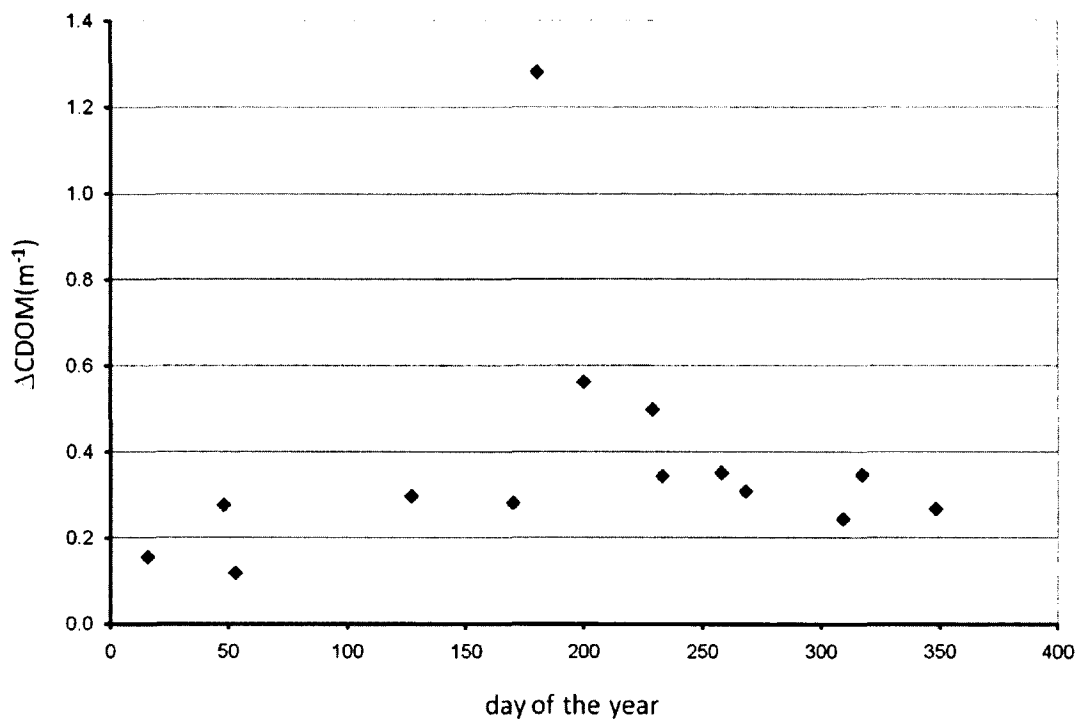


Figure 25. ΔCDOM vs. Julian Day for the 14 COOA Coastal Transect cruises.

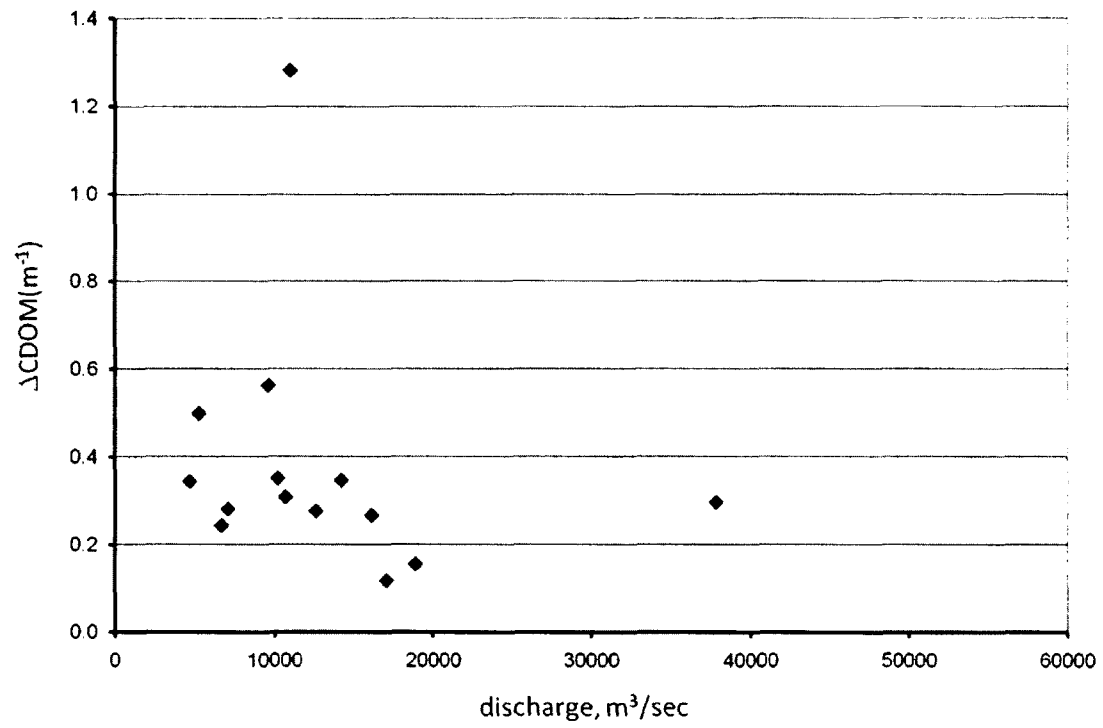


Figure 26. Δ CDOM vs. Daily Discharge for the 14 Coastal Transect cruises.

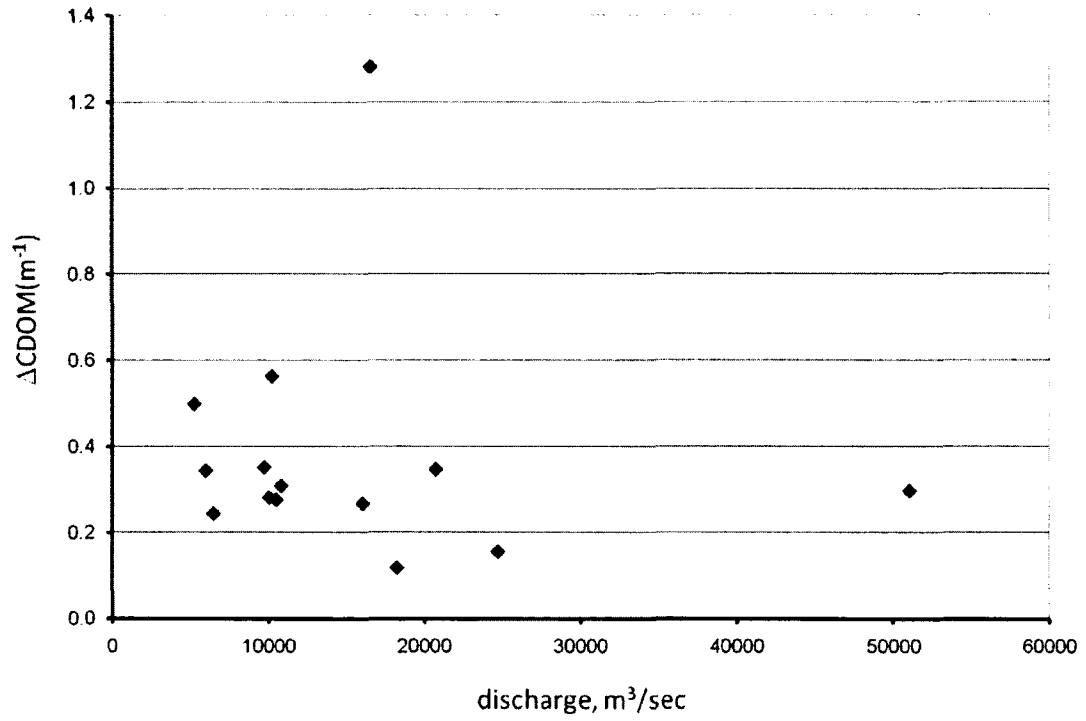


Figure 27. ΔCDOM vs. Average Discharge for the 14 Coastal Transect cruises.

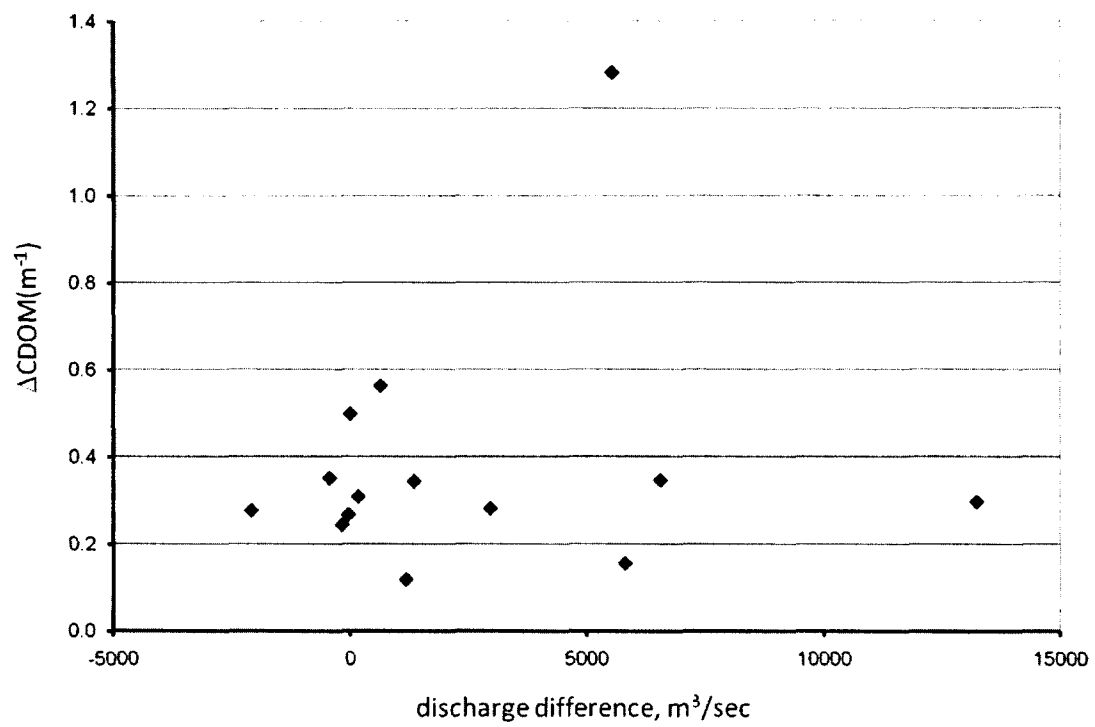


Figure 28. ΔCDOM vs. Discharge Difference for the 14 Coastal Transect cruises.

CHAPTER 4

FINAL WORDS

Originally, the goals of calibrating the CDOM absorption measurements to the continuous fluorescence measurements, and explaining CDOM variability in the Kennebec Estuary were the impetus for this thesis. Although the calibration was surprisingly accurate and successful, attempting to explain CDOM variability was much more complex than anticipated.

The fact that the data showed no obvious trends for factors affecting CDOM variability only reveals the beginning of the complexities surrounding the causes of CDOM variability in an estuary. The lack of a clear direct or inverse relationship between river discharge and CDOM variability in this study begs the possibility of a complex interaction between land processes, discharge, and CDOM that might be deciphered with further investigation. The absence of trends for the factors of discharge and season alludes to the possibility that multiple factors not explored in this research could impact CDOM variability.

The conclusions of this thesis recognize that the complexity of CDOM variability is influenced by numerous factors, and suggest the need for more studies addressing

the causes of CDOM variability. Understanding CDOM variability is an important goal with uses applicable to CDOM remote sensing and freshwater tracing, including the potential to understand DOC flux (Del Castillo and Miller 2008; Mannino et al. 2008; Spencer et al. 2009).

A predictable relationship between CDOM variability and a factor affecting that variability would allow for the prediction of salinity with remotely sensed CDOM. Then CDOM could act as a freshwater tracer, and CDOM remote sensing could trace the freshwater plume. CDOM remote sensing uses ocean color radiance to quantify different CDOM absorption levels. The CDOM slightly discolors the water, and the discoloration changes the radiance values. If CDOM were an accurate freshwater tracer in estuaries, CDOM remote sensing could accurately map freshwater discharge into coastal areas. The uses of FDOM remote sensing in freshwater tracing would also increase, since remotely sensed FDOM measurements can be converted to CDOM data.

Recommendations are for future studies of possible factors affecting CDOM variability in the Kennebec River Estuary. The roles of phytoplankton production, seasonal differences in soil composition in the watershed, and photobleaching of CDOM should be explored for their potential impact on CDOM variability. Additional studies of the influence of salt marsh grass on CDOM accumulation levels could confirm a seasonal connection between salt marsh growth and increased CDOM accumulations in the water. A detailed analysis of tidal influences in the Kennebec Estuary would provide more accurate information regarding the impact of salt marshes on CDOM variability.

Future developments in the use of CDOM as a freshwater tracer in the Kennebec Estuary could involve both *in situ* and remote sensing measurements. A possible future monitoring system would place three optical buoys at the head, center, and mouth of the Kennebec Estuary to take continuous salinity and CDOM readings. Since no predictable relationship between salinity and CDOM variability has been found for this region, these buoys would continuously calibrate CDOM to salinity instead. Remotely sensed CDOM measurements along the entire expanse of the estuary would enhance the buoy data, and permit the derivation of a “CDOM map” of the Kennebec Estuary and its plume. Used in conjunction with the buoy data, the “CDOM map” could essentially map the salinity levels in the Kennebec Estuary, and trace the presence of freshwater entering the Gulf of Maine.

This thesis is one of the first in the department to use the UNH COOA dataset as a primary data source. It also is one of the first in the department to explore CDOM variability and its potential as a freshwater tracer in a coastal system.

References

Blough NV, Del Vecchio R. 2002. Chromophoric DOM in the coastal environment. In: Hansell DA, Carlson CA, editors. Biogeochemistry of marine dissolved organic matter. San Diego: Academic Press. p 509-546.

Blough NV, Green SA. 1995. Spectroscopic characterization and remote sensing of nonliving organic matter. In: Zepp RG, Sonntag Ch., editors. The role of nonliving organic matter in the earth's carbon cycle. Chichester: John Wiley & Sons. p 23-45.

Bricaud A, Morel A, Prieur L. 1981. Absorption by dissolved organic matter of the sea (yellow substance) in the UV and visible domains. *Limnol Oceanogr* 26(1):43-53.

Callahan J, Dai M, Chen RF, Li X, Lu Z, Huang W. 2004. Distribution of dissolved organic matter in the Pearl River Estuary, China. *Mar Chem* 89:211-24.

Carder KL, Steward RG, Harvey GR, Ortner PB. 1989. Marine humic and fulvic acids: their effects on remote sensing of ocean chlorophyll. *Limnol Oceanogr* 34(1):68-81.

Chen RF, Gardner GB. 2004. High-resolution measurements of chromophoric dissolved organic matter in the Mississippi and Atchafalaya River plume regions. *Mar Chem* 89:103-25.

Clark CD, Litz LP, Grant SB. 2008. Salt marshes as a source of chromophoric dissolved organic matter (CDOM) to southern California coastal waters. *Limnol Oceanogr* 53(5):1923-33.

Coble PG. 1996. Characterization of marine and terrestrial DOM in seawater using excitation-emission matrix spectroscopy. *Mar Chem* 51:325-46.

Coble PG. 2007. Marine optical biogeochemistry: the chemistry of ocean color. *Chem Rev* 107:402-18.

Del Castillo CE, Miller RL. 2008. On the use of ocean color remote sensing to measure the transport of dissolved organic carbon by the Mississippi River Plume. *Remote Sens Environ* 112:836-44.

Ferrari GM, Mingazzini M. 1995. Synchronous fluorescence spectra of dissolved organic matter (DOM) of algal origin in marine coastal waters. *Mar Ecol Prog Ser* 125(1-3):305-15.

Gardner GB, Chen RF, Berry A. 2005. High-resolution measurements of chromophoric dissolved organic matter (CDOM) in the Neponset River Estuary, Boston Harbor, MA. *Mar Chem* 96:137-54.

Green SA, Blough NV. 1994. Optical absorption and fluorescence properties of chromophoric dissolved organic matter in natural waters. *Limnol Oceanogr* 39(8):1903-16.

Harvey GR, Boran DA. 1985. Geochemistry of humic substances in seawater. In: Aiken GR, McKnight DM, Wershaw RL, MacCarthy P, editors. *Humic substances in soil, sediment, and water: geochemistry, isolation, and characterization*. New York: John Wiley & Sons. p 233-47.

Helms JR, Stubbins A, Ritchie JD, Minor EC. 2008. Absorption spectral slopes and slope ratios as indicators of molecular weight, source, and photobleaching of chromophoric dissolved organic matter. *Limnol Oceanogr* 53(3):955-69.

Hopkinson CS, Buffam I, Hobbie J, Vallino J, Perdue M, Eversmeyer B, Prahf F, Covert J, Hodson R, Moran MA, Smith E, Baross J, Crump B, Findlay S, Foreman K. 1998. Terrestrial inputs of organic matter to coastal ecosystems: an intercomparison of chemical characteristics and bioavailability. *Biogeochemistry* 43(3):211-34.

Hunt CW. 2002. Spatial and temporal patterns of inorganic nutrient concentrations in the Androscoggin and Kennebec River, Maine. MS Thesis, Department of Earth Science, University of New Hampshire, Durham.

Kirk JTO. 1983. *Light and photosynthesis in aquatic ecosystems*. Cambridge, Great Britain: Cambridge University Press. 401 p.

Liu KK, Atkinson L, Chen CTA, Gao S, Hall J, Macdonald RW, Talaue McManus L, Quinones R. 2000. Exporting continental margin carbon fluxes on a global scale. *EOS Transactions (American Geophysical Union)* 81(52):641.

Mannino A, Russ ME, Hooker SB. 2008. Algorithm development and validation for satellite-derived distributions of DOC and CDOM in the U.S. Middle Atlantic Bight. *J Geophys Res* 113, C07051.

Mitchell BG, Kahru M, Wieland J, Stramska M. 2003. Determination of spectral absorption coefficients of particles, dissolved material and phytoplankton for discrete water samples. In: Mueller JL, Fargion GS, McClain CR, editors. *Ocean optics protocols for satellite ocean color sensor validation. NASA/TM-2003-211621/Rev4-Vol.IV.*

Mitnik PE. 2002. Androscoggin River modeling report and alternative analysis. Maine Department of Environmental Protection, Augusta. DEPLW2001-11.

Nelson NB, Siegel DA. 2002. Chromophoric DOM in the open ocean. In: Hansell DA, Carlson CA, editors. *Biogeochemistry of marine dissolved organic matter*. San Diego: Academic Press. p 547-578.

Romera-Castillo C, Nieto-Cid M, Castro CG, Marrase C, Largier J, Barton ED, Alvarez-Salgado XA. 2011. Fluorescence: absorption coefficient ratio – tracing photochemical and microbial degradation processes affecting coloured dissolved organic matter in a coastal system. *Mar Chem* 125:26-38.

Salisbury JE, Vandemark D, Hunt CW, Campbell JW, McGillis WR, McDowell WH. 2008. Seasonal observations of surface waters in two Gulf of Maine estuary-plume systems: relationships between watershed attributes, optical measurements and surface pCO₂. *Estuar Coast Shelf S* 77:245-52.

Salisbury J, Vandemark D, Hunt C, Campbell J, Jonsson B, Mahadevan A, McGillis W, Xue H. 2009. Episodic riverine influence on surface DIC in the coastal Gulf of Maine. *Estuar Coast Shelf S* 82:108-118.

Salisbury J, Vandemark D, Campbell J, Hunt J, Wisser D, Reul N, Chapron B. Spatial and temporal coherence between Amazon River discharge, salinity, and light absorption by colored organic carbon in western tropical Atlantic surface waters. 2011. *J Geophys Res* 116, C00H02, doi:10.1029/2011JC006989.

Spencer RGM, Aiken GR, Butler KD, Dornblaser MM, Striegl RG, Hernes PJ. 2009. Utilizing chromophoric dissolved organic matter measurements to derive export and reactivity of dissolved organic carbon exported to the Arctic Ocean: a case study of the Yukon River, Alaska. *Geophys Res Lett* 36, L06401.

Stedmon CA, Markager S. 2001. The optics of chromophoric dissolved organic matter (CDOM) in the Greenland Sea: an algorithm for differentiation between marine and terrestrially derived organic matter. *Limnol Oceanogr* 46(8):2087-93.

Twardowski MS, Sullivan JM, Donaghay PL, Zaneveld JRV. 1999. Microscale quantification of the absorption by dissolved and particulate material in coastal waters with an ac-9. *J Atmos Ocean Tech* 16:691-707.

Twardowski MS, Donaghay PL. 2001. Separating *in situ* and terrigenous sources of absorption by dissolved materials in coastal waters. *J Geophys Res* 106(C2):2545-60.

Tzortziou M, Neale PJ, Osburn CL, Megonigal JP, Maie N, Jaffe R. 2008. Tidal marshes as a source of optically and chemically distinctive colored dissolved organic matter in the Chesapeake Bay. *Limnol Oceanogr* 53(1):148-59.

USGS Real-Time Water Data. <http://waterdata.usgs.gov/nwis/rt>

Vodacek A, Blough NV, DeGrandpre MD, Peltzer ET, Nelson RK. 1997. Seasonal variation of CDOM and DOC in the middle Atlantic Bight: terrestrial inputs and photooxidation. *Limnol Oceanogr* 42(4):674-86.

Wang X-C, Litz L, Chen RR, Huang W, Feng P, Altabet MA. 2007. Release of dissolved organic matter during oxic and anoxic decomposition of salt marsh cordgrass. *Mar Chem* 105:309-321.